CHARACTERIZATION OF BINARY OFFSET CARRIER (BOC) SYSTEMS COEXISTING WITH OTHER WIDEBAND SIGNALS

THESIS

John M. Hedenberg, Major, USAF

AFIT/GE/ENG/06-02

DEPARTMENT OF THE AIR FORCE
AIR UNIVERSITY

AIR FORCE INSTITUTE OF TECHNOLOGY

Wright-Patterson Air Force Base, Ohio

The views expressed in this thesis are those of the author and do not reflect the official policy or position of the United States Air Force, Department of Defense, or the U.S. Government.

AFIT/GE/ENG/06-02

CHARACTERIZATION OF BINARY OFFSET CARRIER (BOC) SYSTEMS COEXISTING WITH OTHER WIDEBAND SIGNALS

THESIS

Presented to the Faculty

Department of Electrical and Computer Engineering

Graduate School of Engineering and Management

Air Force Institute of Technology

Air University

Air Education and Training Command

In Partial Fulfillment of the Requirements for the

Degree of Master of Science in Electrical Engineering

John M. Hedenberg, M.B.A., B.S.E.E.

Major, USAF

December 2005

AFIT/GE/ENG/06-02

CHARACTERIZATION OF BINARY OFFSET CARRIER (BOC) SYSTEMS COEXISTING WITH OTHER WIDEBAND SIGNALS

John M. Hedenberg, M.B.A., B.S.E.E.

Major, USAF

Approved:

/signed/	
Dr. Michael A. Temple (Chairman)	Date
/signed/	
Dr. Steven C. Gustafson (Member)	Date
/signed/	
LtCol Stewart L. DeVilbiss, PhD (Member)	Date

AFIT/GE/ENG/06-02

Abstract

Results for the modeling, simulation, and analysis of interference effects that modern wideband signals have on Binary Offset Carrier (BOC) system performance are presented. In particular, BOC performance is characterized using a basic system model and parameters consistent with those of the Global Positioning System (GPS) Military System (M-Code signal). Three modern wideband signals are addressed in this work as potential interferers. These include the direct sequence spread spectrum (DSSS) GPS clear/acquisition code (C/A-Code) signal, the DSSS GPS precision code (P-Code) signal, and an Orthogonal Frequency Division Multiplexed (OFDM) signal, which are all modeled to spectrally coexist within the same bandwidth as the M-Code signal. Interference effects are characterized by comparing the bit error performance of a simulated M-Code system independently and then with the coexisting signal present. The M-Code interference results indicate that the GPS C/A-Code and P-Code signals should not interfere with the M-Code signal at the currently anticipated power levels. Both C/A-Code and P-Code signals can exceed the M-Code received power by over 25 dB before the M-Code system performance shows any degradation. The OFDM interference results indicate that the M-Code system is more sensitive to coexistence with a signal of this type; the M-Code system is significantly degraded with OFDM signals just over 30 dB stronger than the M-Code signal. Simulation results also demonstrate that the M-Code system can be susceptible to the same non-wideband interferers as the C/A-Code and P-Code signals.

Acknowledgments

I would like to express my sincere appreciation to my faculty advisor, Dr. Michael Temple, whose guidance, patience, helpful counsel, and practical suggestions were crucial to the successful outcome of this thesis effort. Thank you for helping me troubleshoot all the mistakes in my simulation and accomplish my goals.

I would also like to express my gratitude and thanks to my wife who has been so understanding during this endeavor. You graciously accepted all the late homework nights, reduced family time, and whining without complaint. You always set a higher bar for me than I set for myself, resulting in a better final product. Along with my wife, I thank my wonderful children for putting up with a "ghost father", especially when they would much rather play games, read books, or wrestle with me.

Finally, I thank my parents for their constant support. I know that I can always count on you both for constant encouragement, "eagle eyes" proofreading, and any other assistance you can give.

John M. Hedenberg

Table of Contents

Page

List of Figures

Page

List of Tables

Page

CHARACTERIZATION OF BINARY OFFSET CARRIER (BOC) SYSTEMS COEXISTING WITH OTHER WIDEBAND SIGNALS

I. Introduction

1.1 Background

Today's electromagnetic environment contains an abundance of communication, radar and navigation signals that coexist in the temporal, spectral, and/or spatial domains. There is a need to ascertain whether newly deployed signals will cause increased interference to existing systems. This work provides modeling, simulation, and analysis of interference effects that modern wideband signals have on Binary Offset Carrier (BOC) system performance. By way of illustration, both the future Global Positioning System (GPS) Military Signal (M-Code) [1] and the European Galileo navigation systems [2] will use BOC(10,5) modulations designed to spectrally coexist with other direct sequence spread spectrum (DSSS) navigation signals. Within this effort, BOC performance is characterized using a basic system model and parameters consistent with those of the GPS Military System (M-Code signal).

Interference effects are characterized by observing changes in simulated M-Code Bit Error Rate (BER) after a coexisting signal is introduced into the channel. The deviations in BER are used as an indicator of potential GPS user accuracy degradation. These interference effects are ascertained using three different interfering signals at varying power levels. For all cases considered, M-Code signal strength is fixed at actual received power levels on the ground. Noise power is then adjusted to achieve the desired

probability of bit error (P_B) for baseline performance. Interfering signals with varying power levels are then introduced and BER is measured until the BER approaches 50%.

The future GPS M-Code signal is designed to coexist with the current (legacy) GPS signals on nearly identical frequency spectra with each using similar spread spectrum coding schemes [1]. Previous research has documented the power spectral density separation between the existing GPS clear/acquisition (C/A) and precision (P) code signals and the future M-Code BOC(10,5) modulation from a frequency separation perspective to validate their coexistence [3]. However, only limited previous work has investigated the actual bit error performance resulting from the coexistence of the existing GPS system with the M-Code.

All interference results presented in this work are provided in support of validating the analysis of M-Code interference with C/A-Code receivers described by Betz [3].

1.1.1 GPS M-Code Signal

In August 1999, the GPS Joint Program Office (JPO) received permission to design and develop modernized space vehicles and M-Code receivers [1]. The motivation for this modernization included: 1) protecting military use of GPS by the US and its allies, 2) preventing the hostile use of GPS, and 3) preserving the peaceful use of civil radio navigation service. This modernization was done by designing a signal that provides functionality, performance, and flexibility for an enhanced military radio navigation service while permitting civilian receivers to continue operation with the same

or better performance as they do today [1]. Due to bandwidth limitations imposed on the new GPS signal, the GPS M-Code was designed to coexist on the same frequency band as the existing GPS signals.

The M-Code signal is spectrally centered on the same L1 and L2 carriers as the legacy GPS signals (1575.42 MHz and 1227.6 MHz, respectively) but is transmitted on two sub-carriers located +/- 10.23 MHz from the center frequencies. The military signal is spectrally displaced from the civil code, enabling the civil signal the possibility of being jammed without disrupting reception of the military signal. Each M-Code signal is Binary Phase Shift Keyed (BPSK) modulated on the L1 and L2 bands prior to being spectrally spread. Further modulation of the M-Code signal uses a Binary Offset Carrier signal with a sub-carrier frequency of 10.23 MHz and a spreading code rate of 5.115×10^6 bits per second. This combination of is denoted as BOC(10.23, 5.115) modulation, which is abbreviated to BOC(10,5) for simplicity.

Currently, the GPS M-Code signal is planned to operate at approximately the same received power levels as the current GPS C/A-Code and P-Code signals. However, increased interest and use throughout military and civilian communities has dictated GPS modernization, which increases received GPS signal power by as much as 20 dB [4]. This increased signal strength in coexisting signals enhances the potential risk of interfering with the M-Code signal. Additionally, the emergence of fourth generation (4G) communications signals for wireless devices using Ultra Wideband (UWB) [5] or Orthogonal Frequency Division Multiplexed (OFDM) techniques [6] all have the future potential of interfering with the M-Code system.

A representative power spectral density (PSD) plot for a BOC(10,5) signal is shown in Figure 1.1. As presented, the PSD plot is shown offset from the actual carrier frequency. The actual M-Code BOC(10,5) signal PSD is centered at GPS L1 and L2 frequencies of 1575.42 MHz and 1227.6 MHz, respectively.

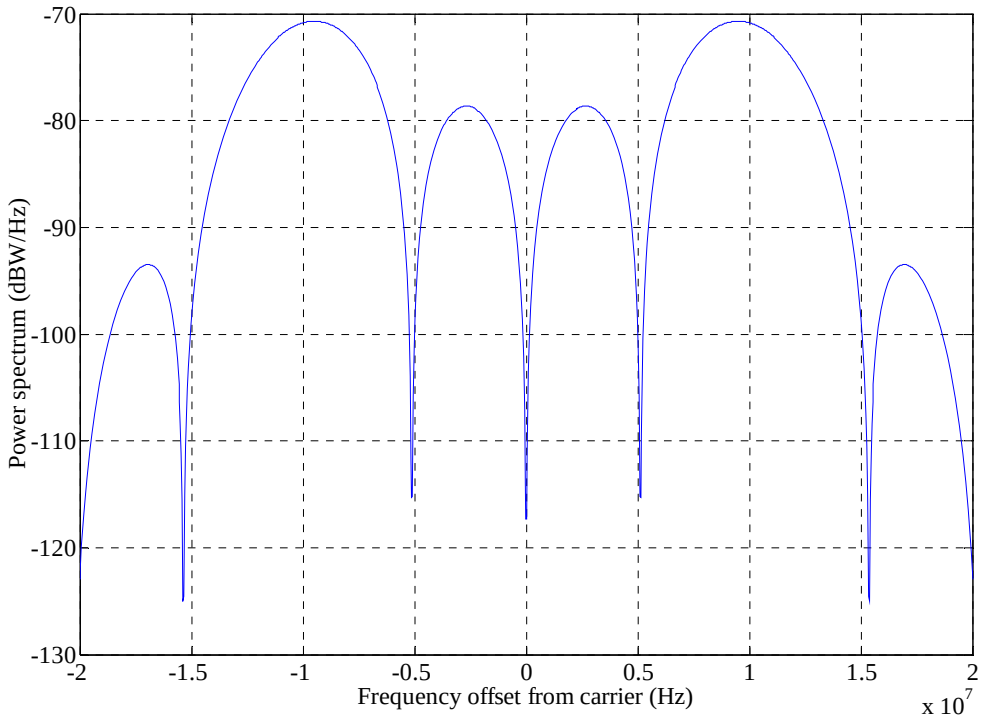

Figure 1.1: PSD of future GPS M-Code BOC(10,5) signal. Amplitude of PSD shown is based on 1.0 W of received power and does *NOT* reflect actual M-Code power levels.

1.1.2 Current GPS Signal

Much has been written about the current Global Positioning System (GPS) system due to its importance in a large number of both military and civil positioning and navigation applications. GPS satellites currently transmit at two carrier frequencies: 1575.42 MHz (L1) and 1226 MHz (L2). There are two independent signals transmitted at each of these frequencies, the clear/acquisition (C/A-Code) and the precision (P-Code) signals, which are both spread spectrally. Both the C/A-Code and P-Code signals are transmitted using Binary Phase Shift Keyed (BPSK) spread spectrum signals. The C/A-Code signal has a chipping rate of 1.023 MHz and the P-Code signal has a chipping rate of 10.23 MHz. These chipping rates create a wide spread of the BPSK signal, permitting significant processing gain (interference suppression) in the receiver.

A 43.0 dB receiver processing gain is achieved for the signal as a result of the large spreading ratios of GPS signals. However, the received satellite signals are very weak, with a given satellite only transmitting about 50 W of Radio Frequency (RF) power. This transmitted power level coupled with long propagation distances results in a minimum received power level (at a ground receiver) for the L1 C/A-Code of approximately -160.0 dBW. The P-Code provides greater processing gain (53.0 dB), but the received signals are slightly weaker (-163.0 dBW and -166.0 dBW minimum power at L1 and L2, respectively).

Figure 1.2 shows representative PSD plots for the C/A-Code and P-Code signals which are centered at GPS L1 and L2 frequencies of 1575.42 MHz and 1227.6 MHz, respectively. As presented, the PSD plot is shown offset from the actual carrier

frequency. The plot in the figure is for a noise-free environment. Due to the very low received power levels, these signals are normally completely masked by thermal noise, i.e., their peak PSD response falls below the "typical" GPS noise floor of –111.0 dBm/MHz. [7]

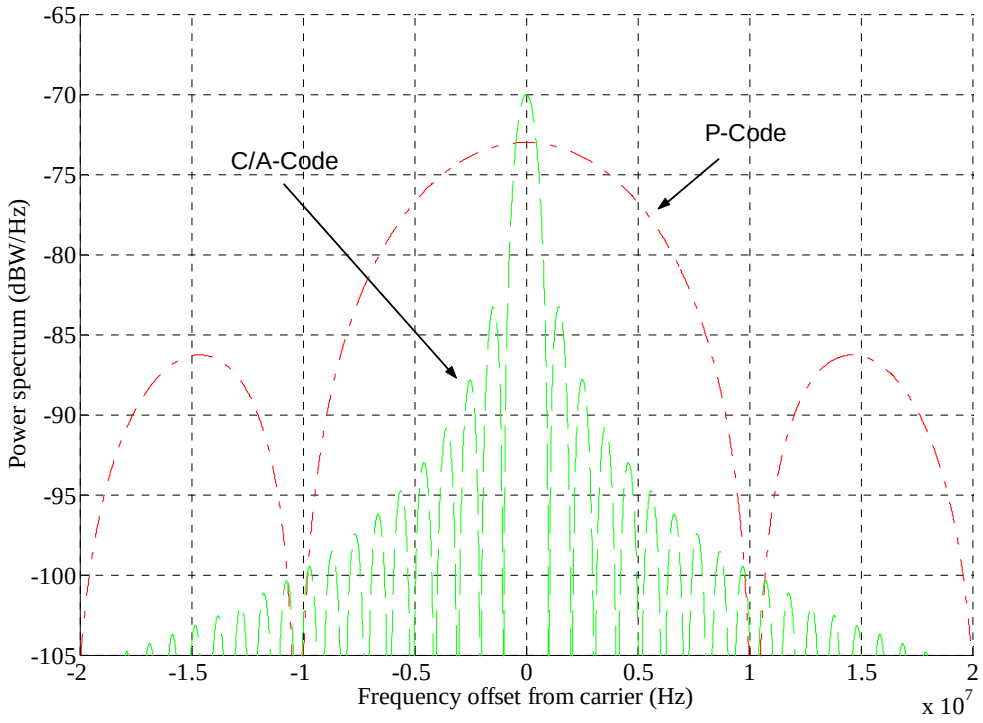

Figure 1.2: PSD of current GPS C/A-Code and P-Code signals. Amplitude of PSD shown is based on 1.0 W of received power and does *NOT* reflect actual received power levels. Note: The C/A-Code signal maximum amplitude is 3.0 dB higher than the P-Code signal maximum.

1.2 Problem Statement

The purpose of this work is to model and simulate the effects (if any) that each of the current C/A-Code and P-Code GPS signals will have on M-Code receiver

performance. Interference effects may occur due to the similar power levels and overlapping spectral location of the current and future GPS signals. Additionally, proposed GPS modernization calls for higher M-Code power levels, which may increase interference to co-existing systems. Simulated BER performance is used to compare M-Code system performance under interference-free, Additive White Gaussian Noise (AWGN) conditions (baseline) with performance results obtained when interfering signals are introduced and interfering power is varied. Noted changes in BER performance are indicative of position accuracy reductions for GPS users.

1.3 Summary of Current Knowledge

The GPS C/A-Code and P-Code signals are a form of Direct Sequence Spread Spectrum (DSSS). DSSS is a digital information transmission technology whereby data sequences (series of bits) at the sending station are combined with a higher rate, independent sequence of bits, or chipping code, that divides the user data according to a spreading ratio. The chipping code is a redundant bit pattern for each bit that is transmitted which increases signal resistance to interference. If one or more bits in the pattern are damaged during transmission, the original data can be recovered due to the redundancy of the transmission.

Understanding the effect of high power M-Code signals on the reception of C/A-Code signals was an important part of the design process used for selecting the final M-Code signal structure. Significant theoretical work was done prior to selecting the BOC(10,5) modulation as waveform of choice [3]. The M-Code development studies

primarily focused on the degradation of idealized receivers for C/A-Code and P-Code while considering interference from similarly powered M-Code signals.

Previous analyses generally considered one channel of a C/A-Code receiver designed for one desired C/A-Code signal. This desired signal was modeled as a known baseband signal (except for unknown delay and phase). The composite received waveform was analyzed as the sum of the C/A-Code signal, thermal noise, and interference from other GPS signals received at the same carrier frequency. The research concluded that the RF interference effect of the M-Code on C/A-Code receiver performance was minimal. In the end, the BOC(10,5) modulation demonstrated best performance over other proposed M-Code signal structures while imposing significantly less degradation in some cases [3].

In contrast to DSSS modulation, frequency division multiplexing (FDM) is an alternate spectral spreading technique whereby multiple independent signals are simultaneously transmitted over a single transmission path, such as a cable or wireless media. In FDM, each independently data (text, voice, video, etc.) modulated signal travels within its own unique frequency range (carrier). Orthogonal FDM (OFDM) is a technique which spreads (distributes) data across a large number of carriers that are spectrally spaced to maintain orthogonality. This orthogonality prevents the demodulators from "seeing" signals at frequencies other than their own. OFDM benefits include high spectral efficiency, resiliency to RF interference, and lower multi-path distortion [8]. These benefits are most useful in typical terrestrial broadcasting applications where multipath channels (i.e., the transmitted signal arrives at the receiver

along various propagation paths having different lengths). Intersymbol interference (ISI) occurs since multiple replicas of the signal interfere, making it more difficult to reliably extract the original information.

OFDM is sometimes called multi-carrier or discrete multi-tone modulation. It is the modulation technique used for digital TV in Europe, Japan, and Australia. In addition, wireless systems such as the 802.11a Wireless Local Area Network (WLAN), 802.16 and WiMAX also use OFDM for fundamental signal transmission.

1.4 Scope

As indicated in Section 1.1.1, the future GPS M-Code signal is to be transmitted in the L1 and L2 bands and is designed to coexist with the existing C/A-Code and P(Y)-Code signals. For this work, coexistence modeling, simulation, and analysis is conducted for all signals located near baseband frequencies. Thus, the effects of receiver RF-to-baseband down-conversion and filtering operations are incorporated. All results are for one M-Code receiver channel which receives a composite signal comprised of the M-Code signal of interest, thermal noise (AWGN), and a single interfering signal.

In addition to using the C/A-Code and P-Code signals as interferers, two additional interfering signals are introduced, including an Orthogonal Frequency Division Multiplexed (OFDM) signal and an actual interfering signal collected insitu at a site in Southern California. The OFDM signal is simulated under worst case conditions whereby the OFDM frequency spectrum totally coexists within the M-Code frequency spectrum. For simulation purposes, the insitu interferer is simulated as a BPSK signal at

power levels closely matching measured results. The purpose of this insitu interfering simulation is to determine if and how this actual signal could degrade M-Code system performance, given that it currently causes severe degradation to civil GPS operation in the local area.

For the C/A-Code, P-Code, and OFDM interfering signals, the received power levels are initially set to match the M-Code signal power and then are gradually increased by as much as 80.0 dB. Simulations are effectively terminated when a BER of 50% is realized. Degradation in BER performance is shown using *Average Interference Power*-to-*Average Signal Power* ratio (I/S) and *Average Signal Power*-to-*Average Interference-plus-Noise Power* Ratio (SINR) analysis. As interfering power is increased, susceptibility and/or rejection capability is demonstrated for the M-Code system for all coexisting interferers considered.

1.5 Thesis Organization

Detailed information on the new GPS M-Code Signal Structure, current GPS signal structures, and other interfering signals are presented in Chapter 2. Chapter 3 provides the simulation methodology and models used for each GPS signal and generated interfering signals. Chapter 4 presents coexistent BER performance results obtained from simulation and analysis. Finally, conclusions and recommendations for future research are presented in Chapter 5.

II. Signal Structure Background

2.1 Overview

This chapter presents detailed information on the five signals considered in this study, including the new GPS M-Code as the signal of interest and four different interfering signals. The interfering signals investigated include: 1) the current GPS C/A-Code signal, 2) the current GPS P-Code signal, 3) an emerging 4G communication signal using OFDM, and 4) an actual interfering signal collected insitu at a site in Southern California which is modeled as a BPSK signal. The focus is on signal generation and structure of the new M-Code as compared to all interfering signals. While there are many different types of waveforms that could be considered, this work primarily pertains to signals that will spectrally coexist with the new M-Code signal in/around the L1 and L2 frequency bands. Specifically, this chapter focuses on the specific PSD structure and relative power levels of the different signals.

2.2 New GPS M-Code Signal

The new GPS M-Code signal was designed to accomplish specific upgrade goals, including [10]: 1) better jamming resistance than current P-Code signals as accomplished through higher transmit power while inducing minimal interference to existing C/A-Code or P-Code operations, 2) compatibility with prevention jamming against enemy GPS use, 3) more robust signal acquisition, 4) comparable, perhaps better, performance than the P-Code signal, 5) coexistence with current signals operating at/near L1 and L2 frequencies

while not interfering with current or future military user equipment, and 6) simple and low risk implementation on both space vehicles and future equipment (must be as power efficient as possible).

The main desired criteria for choosing an M-Code modulation scheme has a majority of the power displaced from the carrier frequency (f_c) and concentrated at ± 10.23 MHz about f_c. The BOC(10,5) modulation is selected as the technical solution best meeting these requirements. Since the BOC spreading waveform has an average value of zero, its spectrum has a null at the band center. Also, since the dominant variation in the BOC spreading waveform occurs at a higher rate than the spreading code applied, most of the BOC(10,5) power occurs at frequencies higher than the spreading code rate. Since the BOC(10,5) spectrum is distinct from that of the C/A-Code and P-Code signals, the BOC(10,5) modulation can be received at relatively high power levels without degrading C/A-Code or P-Code receiver performance.

The M-Code Power Spectral Density (PSD) can be analytically expressed by [1]

$$G_{BOC(fs,fc)}(f) = f_c \left\{ \frac{\sin\left(\frac{\pi f}{2 f_s}\right)\sin\left(\frac{\pi f}{f_c}\right)}{\pi f \cos\left(\frac{\pi f}{2 f_s}\right)} \right\}^2, \qquad (2.1)$$

where $f_s = 10.23 \times 10^6$ Hz and $f_c = 5.115 \times 10^6$ Hz are the specific parameters chosen for M-Code implementation. Figure 2.1 shows an overlay of the baseband PSDs for the current C/A-Code signal (green dashed line), P-Code signal (red dot-dashed line), and the new M-Code signal (blue solid line) in a noise-free environment. Normally, these signal

PSDs are hidden by the thermal noise floor. It is evident in these spectral overlay plots that the potential for coexistence interference exists.

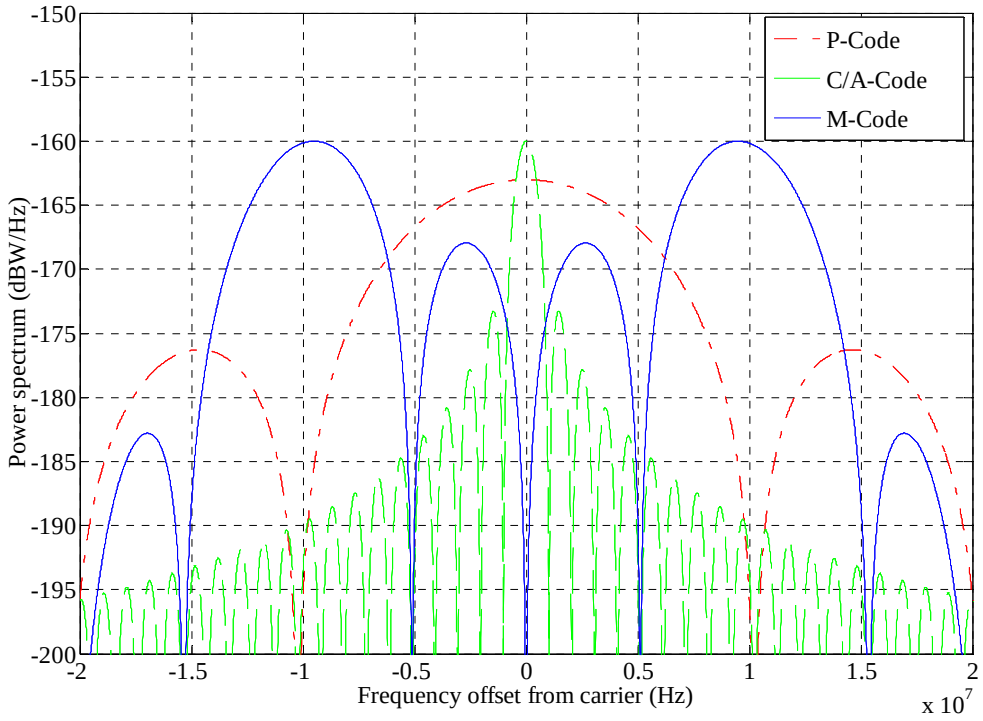

Figure 2.1: PSDs of coexisting C/A-Code, P-Code, and M-Code signals. The PSD will be centered on both the GPS L1 and L2 carrier frequencies.

Transmission of the M-Code signal at higher power levels without degrading existing system performance is one of the key design goals of M-Code implementation [3]. As seen in Figure 2.1, the M-Code peak spectral responses at ± 10.23 MHz are effectively displaced from the current GPS signal PSD peak responses. However, there is an obvious overlap of M-Code side lobe responses and the P-Code response throughout the spectrum. Table 2.1 shows minimum and maximum received RF signal power levels for the M-Code listed by the satellite production version [11].

Table 2.1: Received RF M-Code Signal Strength [11]

Production Version	Min (dBW)	Max (dBW)
Block IIF	-160	-153
Block IIR-M	-160	-153
Future SVs	-158	-131

2.3 Current GPS Signals

Current GPS satellite signals are transmitted on two separate carriers located at 1575.42 MHz (designated L1) and 1227.6 MHz (designated L2). Two Direct Sequence Spread-Spectrum (DSSS) Binary Phase Shift Keyed (BPSK) modulated signals are on the L1 frequency band. The first is the Coarse/Acquisition (C/A)-Code, which has a chipping rate of 1.023 MHz. The second is the Precise (P)-Code, which has a chipping rate of 10.23 MHz. The C/A-Code is unencrypted and is used by all GPS receivers to accomplish initial signal acquisition. For civilian applications, the C/A-Code is the only signal available for position estimation. The P-Code is encrypted to provide anti-spoofing capability and is denoted as the P(Y)-Code. For military applications, the C/A-Code is used for acquisition prior to using the encrypted P(Y)-Code for positioning.

Each GPS satellite generates a 50 bit/second navigation message based upon data periodically uploaded from the GPS Control Segment and adds the message to the 1.023 MHz Pseudo Random Noise (PRN) C/A-Code sequence. The navigation message consists of data bits which describe the GPS satellite orbits, clock corrections, ionospheric propagation delay, and other system parameters. The satellite modulates the

resulting code sequence onto the L-band carrier to create a spread spectrum ranging signal which is broadcast to the user community. Each satellite is assigned a unique C/A-Code which provides the mechanism for identifying each satellite within the constellation. The GPS satellite also transmits a second spread spectrum ranging signal known on L2 which supports Precise Positioning System (PPS) user two-frequency corrections [12]. Figure 2.2 [13] illustrates the signal generation process used for the transmitted C/A-Code on L1.

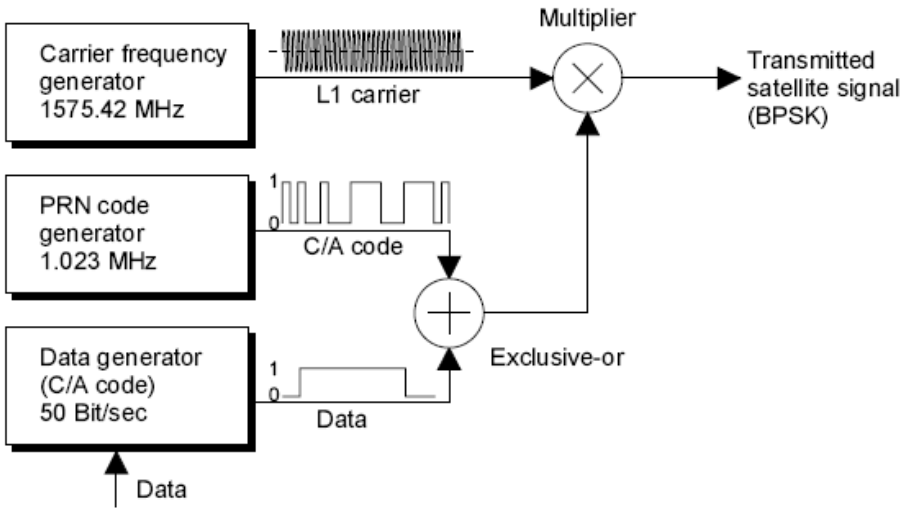

Figure 2.2: Block diagram of GPS C/A-Code signal generation on L1 [13]. The P-Code signal generation is accomplished using a PRN Code generator with a frequency of 10.23 MHz. The C/A-Code and P-Code signals are likewise generated for L2 through using a carrier frequency of 1227.6 MHz.

Although generation of the C/A-Code and P-Code signals is accomplished through identical procedures, the relative power levels of the two signals differ between the L1 and L2 as documented in Table 2.2.

Table 2.2: Minimum Received Signal Strength of Current GPS Signals [4]

Frequency Band	Signal Power (dBW)	
	P	C/A
L1	-163	-160
L2	-166	-166

Before proceeding with GPS signal analysis, it is important to understand how the GPS signal is generated at the bit level. Figure 2.3 [13] depicts the generation process for the GPS C/A-Code signal on L1 from independent signal inputs. The 50 bit/s data stream is modulated with the C/A-Code stream to produce the spread, data modulated waveform. This waveform is then modulated onto the L1 carrier signal to produce the transmitted BPSK modulated carrier signal. The P-Code and L2 signals are generated via a similar process.

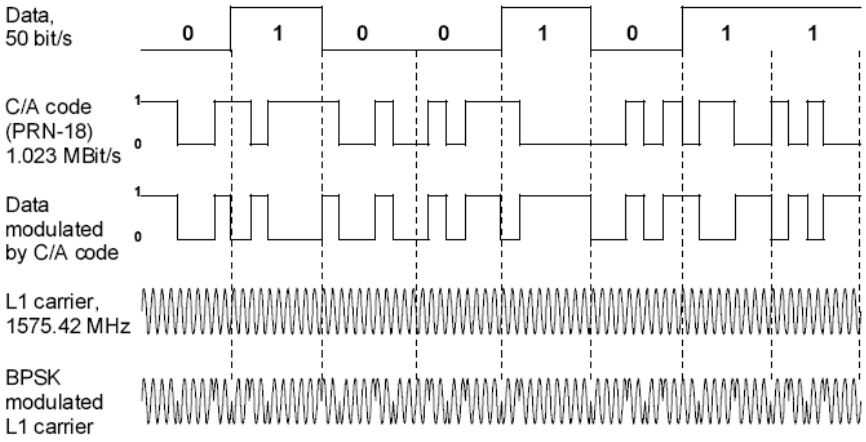

Figure 2.3: Bit level representation of transmitted GPS BPSK C/A-Code signal [13] . The P-Code signal generation is accomplished using a PRN code generator with a frequency of 10.23 MHz. The C/A-Code and P-Code signals are likewise

generated for L2 using a carrier frequency of 1227.6 MHz.

2.3.1 Current C/A-Code Signal

The C/A-Code consists of a 1023 bit PRN code at a clock rate of 1.023 MHz which repeats periodically every 1.0 millisecond. This noise-like PRN code modulates the L1 carrier signal and effectively "spreads" the signal spectrum over a 1.023 MHz bandwidth. The relatively short period of the C/A-Code is designed to enable a receiver to rapidly acquire the satellite signals, which helps the receiver transition in acquiring and tracking the longer P-Code. A unique PRN code is assigned to each GPS satellite and is selected from a set of Gold Codes. Gold Codes are designed to minimize the probability that a receiver will mistake one code for another (minimizes cross-correlation). The C/A-Code is only transmitted on L1 and is not encrypted. Therefore, it is available to all GPS users independent of application [14].

2.3.2 Current P-Code Signal

The P-Code is a 10.23 MHz PRN Code sequence having a period of 267 days. Each GPS satellite is assigned a unique seven-day segment P-Code that restarts every Saturday/Sunday midnight GPS time (GPS time is a continuous time scale maintained within 1.0 microsecond of Coordinated Universal Time (UTC), plus or minus an integer number of leap seconds). The P-Code is normally encrypted into the Y-Code to protect the user from spoofing. Given GPS satellites have the capability to transmit either the unencrypted P-Code or encrypted P(Y)-Code. The P(Y)-Code is transmitted by each satellite on both L1 and L2. The transmitted P(Y)-Code on L1 is 90 degrees out-of-phase

with the C/A-Code carrier [14]. The encrypted P(Y)-Code requires a classified Anti-Spoofing (AS) Module for each receiver channel and is intended for use by authorized users having cryptographic keys. The P(Y)-Code is the basis for the PPS.

2.4 Additional Interfering Signals

In addition to considering the coexistent effects of current GPS C/A-Code and P-Code signals on M-Code system performance, two additional interfering signals were investigated. The first is an Orthogonal Frequency Division Multiplexed (OFDM) signal similar to what is used in 3G communications (e.g., 802.11 wireless devices) and what is proposed for 4G communications systems. The OFDM signal was simulated for a worst case scenario in which the coexisting OFDM frequency spectrum is totally coincident with the M-Code frequency spectrum.

The second non-GPS interfering signal was modeled based on experimental data collected for an actual signal shown to significantly degrade current GPS L1 signal reception and accuracy. In this case, the experimental interfering data was collected insitu in the Southern California vicinity. Although the actual signal structure for this interferer was deemed "unknown," the signal was modeled as a randomly modulated BPSK signal based on RF measurements. The simulated relative power level and frequency span of the interfering signal were set to be consistent with measured data.

2.4.1 Orthogonal Frequency Division Multiplexing (OFDM)

Orthogonal Frequency Division Multiplexing (OFDM) is a modulation and/or multiplexing technique which spectrally divides a communication channel into a number of equally spaced frequency bands. Each OFDM subcarrier carries a portion of user information which is transmitted in each band. By design and appropriate parameter selection, each subcarrier is mutually orthogonal to every other subcarrier, which minimizes interference between subcarriers. The OFDM is sometimes referred to as multi-carrier or discrete multi-tone modulation. An OFDM-based system divides a high-speed serial information signal (bit stream) into multiple lower-speed sub-signals that the system transmits simultaneously over different frequencies in parallel.

Benefits of OFDM include: 1) high spectral efficiency, 2) resiliency to RF interference, and 3) lower multi-path distortion. The orthogonal nature of OFDM allows subchannels to overlap, which has a positive effect on spectral efficiency (see Figure 2.4).

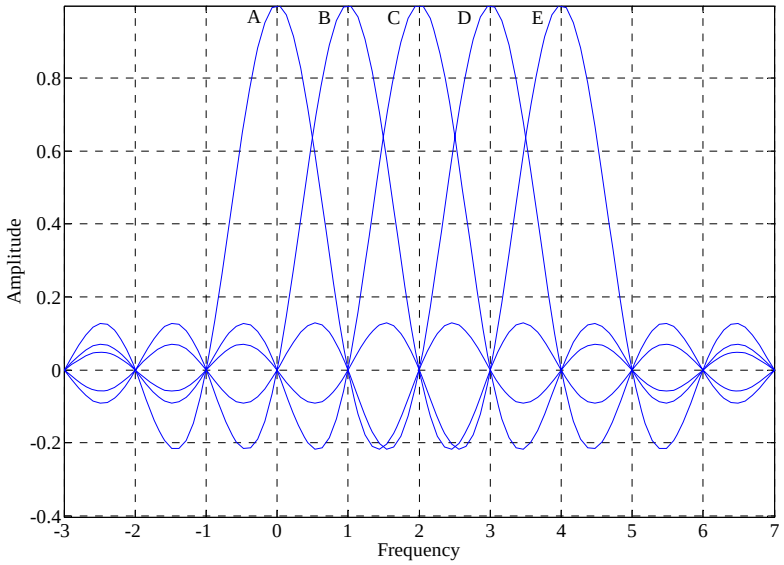

Figure 2.4: Spectral response of an OFDM signal with five subcarriers. The

subcarriers A, B, C, D, and E are shown at an arbitrary power amplitude and frequency. By definition, OFDM subcarriers are mutually orthogonal, avoiding interference with each other. The subcarrier frequency overlap minimizes the overall amount of spectrum required.

Obviously, the subcarrier spectral responses are not completely separated and thus overlap. However, the information transmitted over the carriers can still be separated given the orthogonality signal relationship for which the method is named. Using an Inverse Fast Fourier Transform (IFFT) for modulation, the subcarrier spacing is implicitly chosen such that all other signals are zero at frequencies where the received signals (indicated as the letters A-E) are evaluated.

This parallel-form of transmission over multiple subcarriers enables OFDM-based WLANs to operate at higher aggregate data rates, e.g., up to 54 Mbps is achieved in IEEE 802.11a-compliant implementations [9]. From a spectral perspective, in operational environments where interfering RF signals only coexist with a portion of the OFDM signal, there is inherent interference suppression. From a temporal perspective, OFDM signals exhibit lower multi-path distortion (delay spread), since the high-speed sub-signals are sent at lower data rates. Because of the lower data rate transmissions, multi-path-based delays are not nearly as significant as they would be with a single-channel high-rate system.

Many wired and wireless standard communities have adopted OFDM for a variety of applications. For example, OFDM is the basis for the global standard for asymmetric digital subscriber line (ADSL) and for digital audio broadcasting (DAB) in the European

market [9]. In the wireless network space, OFDM is at the heart of IEEE 802.11a and HiperLAN/2 [9].

The wireless network industry has grown significantly over recent years and there are many established and startup companies developing high-speed wireless network products for wireless multimedia applications. The higher data rates and robust communications of OFDM enable the implementation of WLANs and Metropolitan Area Networks (MANs) supporting higher-speed applications operating over wider areas where the environment is somewhat more “hostile” toward radio transmissions.

An ideal application for OFDM is wireless point-to-point and point-to-multipoint configurations with most initial OFDM products providing this capability. Many wireless MAN products based on OFDM began appearing on the market in early 2001. A problem with implementing WLAN products based on OFDM is the limited range they exhibit because of high operating frequency combined with relatively low power.

The IEEE 802.11a standard [14] specifies an OFDM physical layer that splits an information signal across 52 separate subcarriers to provide transmission of data at a rate of 6, 9, 12, 18, 24, 36, 48, or 54 Mbps. The 6, 12, and 24-Mbps data rates are mandatory for all products. Four of the subcarriers are pilot subcarriers that the system uses as a reference to disregard frequency or phase shifts of the signal during transmission. A pseudo binary sequence is sent through the pilot subchannels to prevent the generation of spectral lines. The remaining 48 subcarriers provide separate wireless pathways for

sending the information in a parallel fashion. The resulting subcarrier frequency spacing is 0.3125 MHz (for a 20 MHz total bandwidth with 64 possible sub-carrier frequency slots). Operating frequencies for the 802.11a OFDM layer are in the following three 100-MHz unlicensed national information (UNI) structure bands: 5.15 to 5.25 GHz, 5.25 to 5.35 GHz, and 5.725 to 5.825 GHz [14]. While none of these bands currently overlap with the GPS transmission frequencies, as the use of OFDM through 802.11 technologies increases, future 802.11 bandwidths may encroach on the GPS M-Code signal frequency domain.

2.4.2 Observed Interfering Signal

The fourth coexisting signal investigated in this research is an observed signal collected insitu at a site in Southern California. This coexisting signal currently causes so much interference that GPS L1 C/A-Code and P-Code receiver performance is degraded to the extent that there is a *total loss* of the L1 GPS signals currently received within the immediate vicinity of the transmitter. The specific transmitted signal characteristics of this interfering signal are unknown. However, Figure 2.5 shows a plot of the received spectrum from this transmitter. As can be seen, the peak response of the interfering signal is located approximately 4.0 MHz above the GPS L1 center frequency of 1575.42 MHz and has a magnitude that is approximately 45.0 dB above the L-Band noise floor.

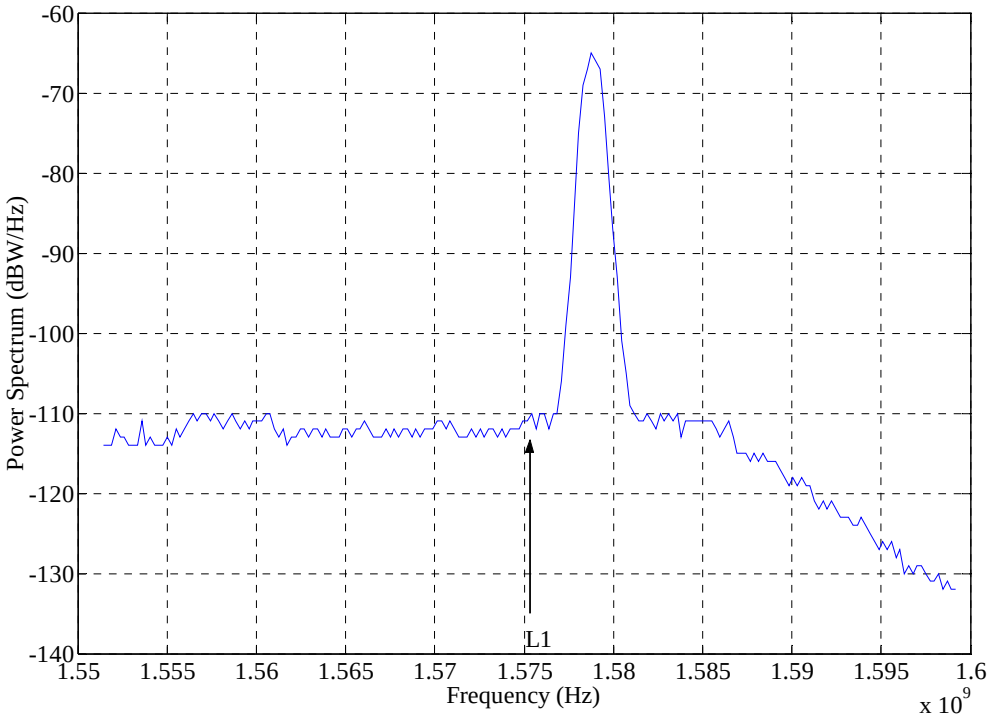

Figure 2.5: Received power spectrum of actual GPS L1 interfering signal. The center of interfering signal is approximately 4.0 MHz above the GPS L1 center frequency of 1575.42 MHz. The peak amplitude of received signal is approximately 45.0 dB above the L1 noise floor.

Multiple observations show that this signal corrupts the current GPS signals on L1. What is currently unknown is whether or not a signal with these characteristics will likewise degrade the future M-Code signal.

2.5 Summary

The effects of four different interfering signals that may coexist in the same frequency range as the future GPS M-Code are independently investigated to determine potential interference effects. The four interfering signals considered include: 1) the

current GPS C/A-Code signal, 2) the current GPS P-Code signal, 3) a worst-case OFDM interfering signal, and 3) an actual observed GPS interfering signal collected insitu in Southern California. A short historical discussion of the future M-Code signal development was presented, as well as a process for generating of both the original GPS signals and an OFDM signal. This information provides the theoretical and conceptual basis used for the simulation methodology, results, and analysis presented in the following chapters.

III. Simulation Methodology and Validation

3.1 Overview

To successfully model interference effects on an M-Code communication system, an M-Code system model was developed, tested, and verified. The model was verified by comparing simulated bit error performance (P_B) for various E_b/N_o values with theoretical BPSK performance given by [15]:

$$P_B = Q\left(\sqrt{\frac{2E_b}{N_o}} \right), \tag{3.1}$$

where E_b is average energy per bit and N_o is the noise power spectral density.

With a BPSK system, the E_b/N_o is proportional to Signal-to-Noise Ratio (SNR) with equality achieved under specific design conditions. This equality can be demonstrated by manipulating common definitions for average signal power (S_{AV}) and average noise power (N_{AV}). In a BPSK modulated system, S_{AV} can be expressed as [15]

$$S_{AV} = \frac{E_s}{T_s} = E_s \cdot R_s = (k \cdot E_b) \cdot (R_D / k) = E_b \cdot R_D , \tag{3.2}$$

where E_s is average energy per symbol, T_s is symbol duration, R_s is symbol rate, and there are k bits per communication symbol ($k = 1$ for BPSK). Using a bandwidth of $W = R_D$, N_{AV} can be expressed as

$$N_{AV} = N_o \cdot W = N_o \cdot R_D . \tag{3.3}$$

Forming SNR as the ratio of (3.2) and (3.3) demonstrates E_b/N_o equality as follows:

$$SNR = \frac{S_{AV}}{N_{Av}} = \frac{E_b \cdot R_D}{N_o \cdot R_D} = \frac{E_b}{N_o}. \quad (3.4)$$

Although the future M-Code signal will be transmitted on the L1 and L2 frequencies of 1575.42 MHz and 1227.6 MHz, the models, simulations and analysis of this work are based on a down-converted M-Code received frequency of 20.23 MHz. This deviation from using actual transmission frequencies in the simulation is due to processing limitations of the PC based MATLAB program. Such a down-conversion from actual M-Code operational frequencies is common and easily accomplished through mixing and filtering operations at the receiver. All interfering signals were generated at or near this down-converted center frequency as well. As illustrated in Figure 3.1, this choice of simulated center frequency ensures that the two the primary side lobes of the M-Code signal are received with minimal distortion. The PSD for the received simulated M-Code signal in Figure 3.1 is for the case with no AWGN or interference present. By comparison with the theoretical M-Code BOC(10,5) PSD presented in Figure 1.1, the simulated M-Code signal was deemed sufficient for reliable communication system performance analysis and subsequent coexistent interference characterization.

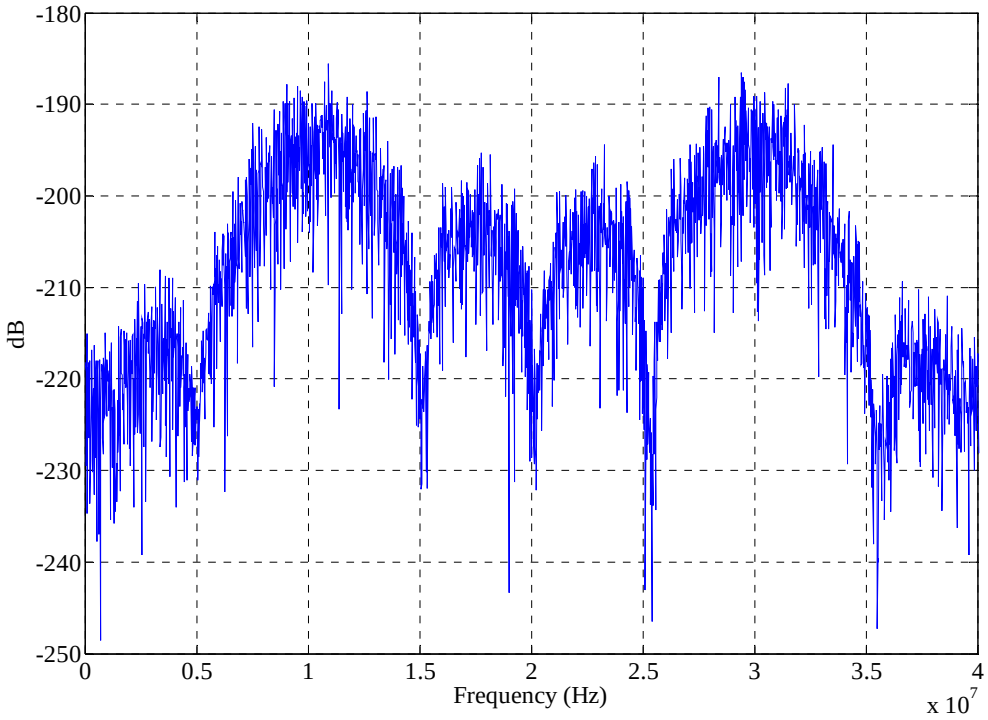

Figure 3.1: PSD of simulated M-Code signal. The simulated M-Code signal is centered at 20.23 MHz rather than the GPS L1 and L2 carriers, located at 1575.42 MHz and 1227.6 MHz. This figure denotes the M-Code signal in a noise free environment without any interfering signals present.

Due to processing limitations, the data rate of the M-Code signal was increased from an actual rate of 50 or 200 bits/second to a value of $R_c/250 = 5.115\times10^6/250 =$ 20,460 bits/second. With appropriate scaling of simulated filter bandwidths, this increase in data rate does not affect the error performance validation of the simulation; it simply speeds up the error accumulation subroutines by speeding up the message bit throughput of the transmission system.

3.2 Interference Analysis Model

Once the M-Code signal model was verified, the SNR ratio was fixed at a specific value and various coexisting signals were introduced into the environment. The coexisting GPS and OFDM signals were initially introduced at relatively low power levels and progressively increased until P_B reached 50% (the point at which the BPSK signal is virtually unrecoverable). For the observed insitu interfering signal, the one which currently interferes with C/A-Code and P-Code receivers, the signal was introduced at a fixed power level based on observed/collected power levels as shown in Figure 2.5. The *Average Interference Power*-to-*Average Signal Power* (*I/S*) and *Average Signal Power*-to-*Average Interference-plus-Noise Power* (SINR) ratios were used for analysis.

3.2.1 Simulated M-Code System Model

The first step in developing a model to evaluate interference effects of coexisting signals with the M-Code signal was to simulate M-Code communication system performance. Given that no specific M-Code system was available for modeling, a simulated transmitter-receiver system was developed using common communication engineering principles (e.g., RF/IF filtering, up/down-conversion, equal energy signaling, coherent/matched filter detection, etc.). Due to limitations on public availability of the M-Code actual p.r.n. code, the simulation uses a random sequence for this function. This substitution does not impact the simulation results and prevents possible data

classification/security concern. Figure 3.2 shows the block diagram of the M-Code system developed for simulation and analysis.

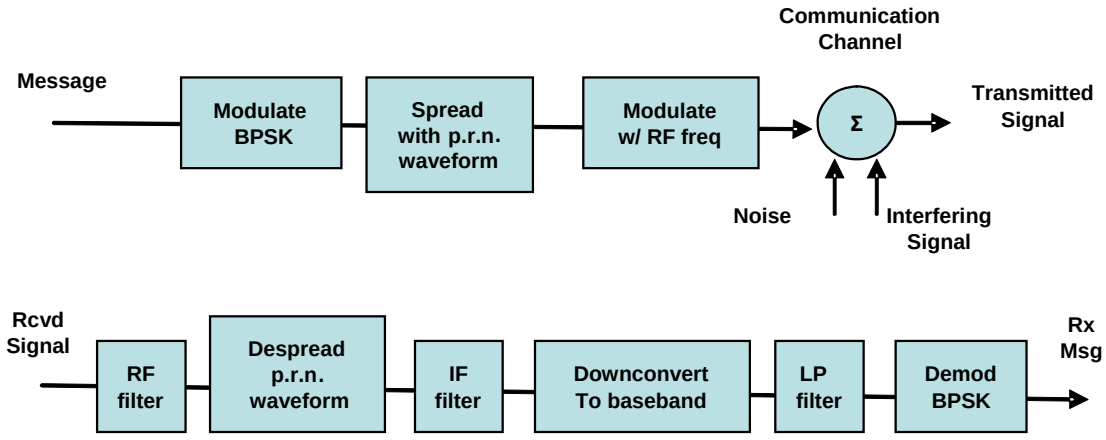

Figure 3.2: Block diagram of M-Code system developed for simulation and analysis. Block diagram shows the M-Code basic message being modulated BPSK, spread with the pseudorandom-noise waveform, and finally modulated on the RF frequency prior to transmission. Additive Gaussian Noise (AWGN) is used to incorporate thermal noise effects. The received signal was filtered and despread prior to BPSK demodulating.

The transmitted M-Code signal can be represented by [17]

$$S_M(t) = \sqrt{2P_M}\, d_M(t) SW(t) PN_5(t) \cos\left(\omega_{L1,L2} t + \theta\right), \tag{3.5}$$

where P_M is M-Code signal power, $d_M(t)$ is the M-Code data modulated waveform, $SW(t)$ is the 10.23 MHz square wave carrier, $PN_5(t)$ is the 5.115 MHz pseudorandom code, $\omega_{L1,L2}$ are the angular L1 and L2 carrier frequencies, and θ is phase.

The following process for generating the received M-Code signal is based on commonly used signal generation architectures [15]. A randomly generated 15 bit M-Code data message at the given data rate is BPSK modulated and then digitally multiplied by a 10.23 MHz square wave carrier and a random binary sequence with a rate of 250

chips/T_D (simulating a pseudorandom code). Finally, IF/baseband carrier modulation at 20.23 MHz is used to generate the down-converted M-Code signal in the receiver. The received power of the M-Code signal is set at the IF/baseband filter output to match actual received power levels described in Table 2.1. The received M-Code signal is first filtered by an RF filter centered at 20.23 MHz, the RF center frequency, with a bandwidth of 20.23 MHz. As shown in Figure 3.3, this bandwidth was determined to be best for maximizing M-Code SNR at the RF filter output.

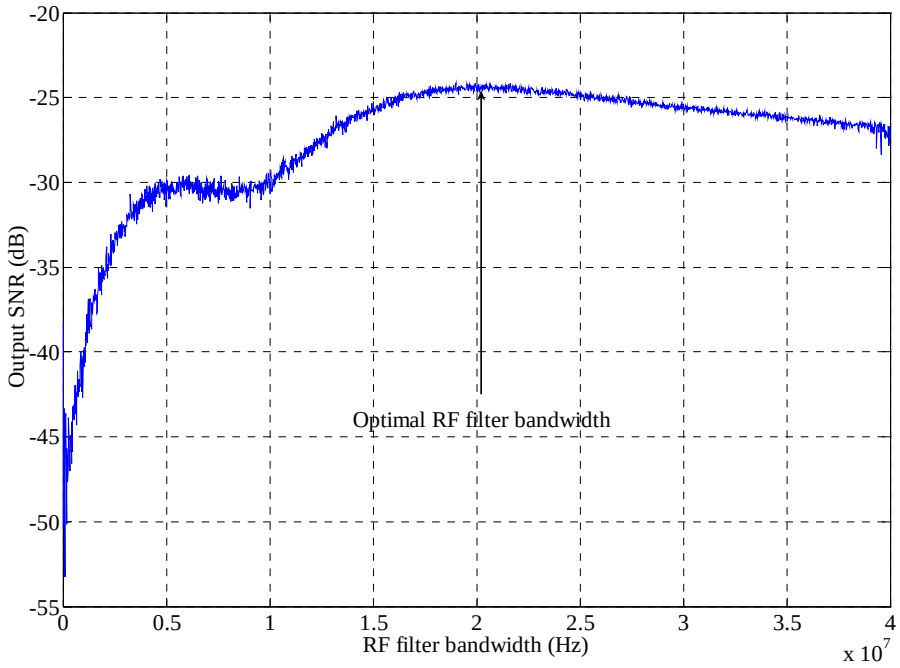

Figure 3.3: SNR response to increasing RF filter bandwidth. The SNR response is maximized at 20.23 MHz. The amplitude of the PSD shown is based on 1.0W of received power and does *NOT* reflect actual M-Code power levels.

The signal was then despread with the original pseudorandom waveform used to modulate the BPSK transmission. The despread signal is next filtered again through an

"IF" filter centered at 20.23 MHz with a bandwidth of 20.460 kHz, the simulation data rate. The signal is then downconverted to baseband and filtered through a final low pass filter using a bandwidth of the data rate. The resulting signal is demodulated, and a bit-by-bit comparison is made with the original transmitted data to generate and estimated P_B. The effects of increasing interfering signal power were observed in estimating P_B by dividing the total number of accumulated bit errors by the total number of bits transmitted through the system. The process was repeated until the number of accumulated errors surpassed a preset value of 5000 to ensure statistical accuracy of the bit error rate.

After developing an M-Code communication system, the next step was to consider the effects of having the interference present during threshold determination. To analyze the effects, a baseline SNR curve for the M-Code system, with no interference present, was first generated as shown in Figure 3.4. Figure 3.4 compares simulated and theoretical P_B for a BPSK signal as the signal-to-noise level increases. The close tracking of the simulated points to the theoretical curve validates the communication performance of the M-Code model.

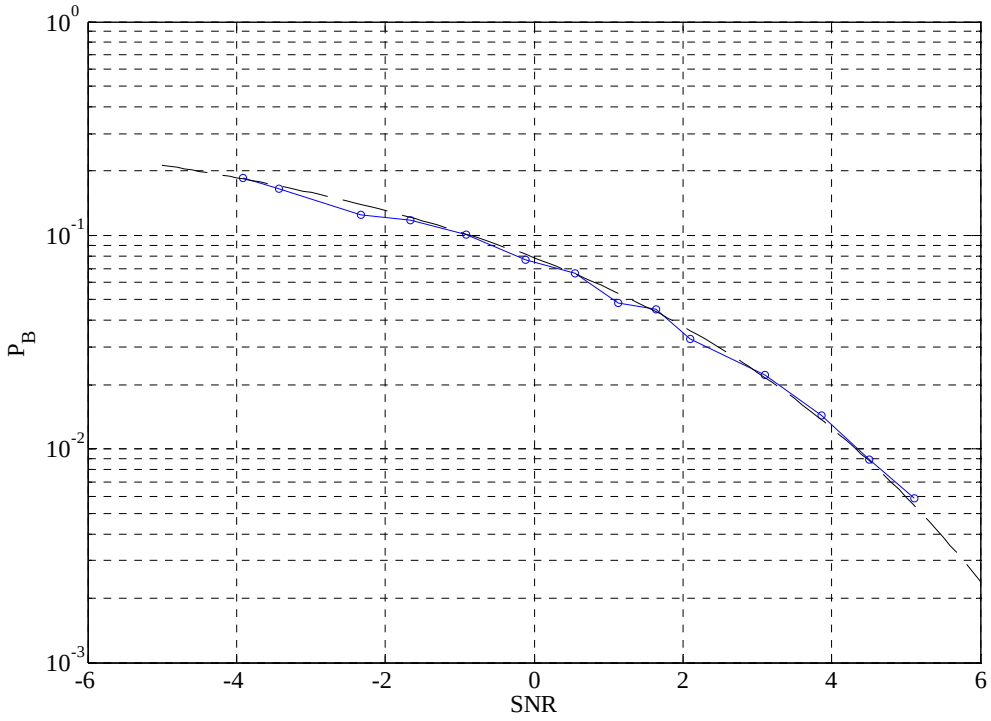

Figure 3.4: The SNR vs. P_B curve for the M-Code transmitter-receiver model. The model covers 9.0 dB SNR range, comparing results to theoretical bit error curve for a BPSK system generated per (3.1).

3.2.2 Simulated Current GPS Signal Model

The first coexisting existing signal that was simulated as a potential interferer was the current GPS C/A-Code signal. This signal was generated as depicted in Figure 3.5. The coexisting signal was generated with a random binary message which was BPSK modulated. The BPSK data modulated signal was then spread with a pseudorandom binary waveform at a 10.23 MHz chip rate. The spread BPSK signal was finally modulated to 20.23 MHz, the same center frequency as the simulated M-Code signal.

This signal was inserted into the M-Code system as one of the interfering signals as shown in Figure 3.2.

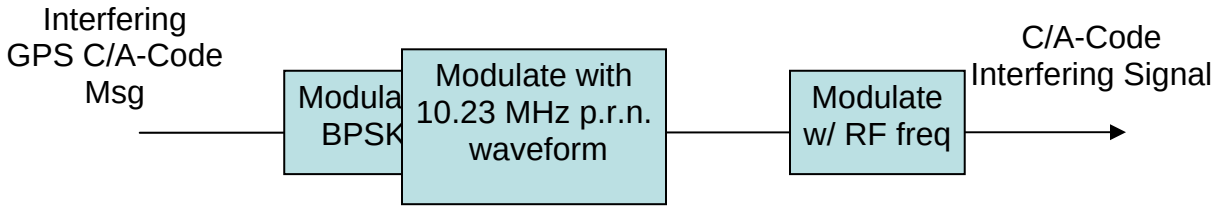

Figure 3.5: Block diagram of GPS C/A-Code interference generation. The 10.23 MHz pseudorandom noise chip rate reflects the actual bandwidth generated by the GPS satellites in orbit. The simulated C/A-Code was modulated to an RF frequency of 20.23 MHz, which is the same center frequency as the simulated M-Code signal.

The C/A-Code interfering signal was initially modeled as spectrally coexisting and having the same received power as the M-Code signal. The C/A-Code interfering power was progressively increased in 2.0 dB steps until it was a total of 80.0 dB above the received M-Code signal level. Figure 3.6 depicts the worst case overlay of the power spectral densities of the M-Code signal and the GPS C/A-Code interferer when the interfering signal is received with the +80.0 dB power level. The BOC(10,5) M-Code signal design places a spectral null at the peak PSD response of the C/A-Code signal. This designed interference avoidance mechanism complements the inherent interference rejection afforded by direct sequence spread spectrum processing and enhances overall system robustness.

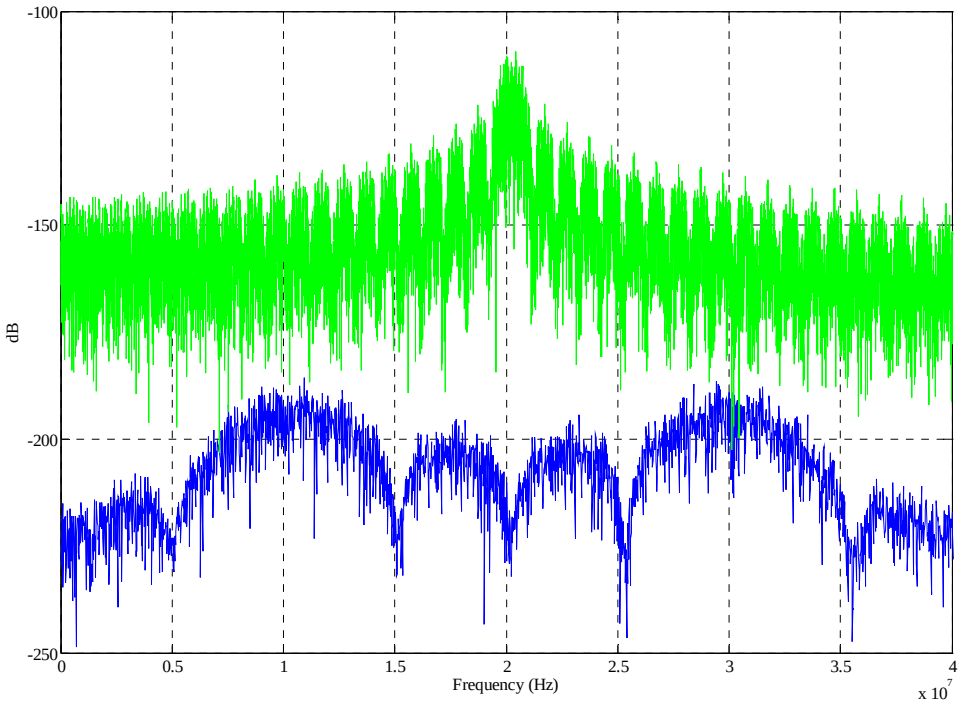

Figure 3.6: The PSDs of the M-Code signal (lower plot) and the coexisting C/A-Code signal (upper plot). Relative power levels depicted in this figure are for a worst case interfering scenario where the received C/A-Code signal power is 80.0 dB above the received M-Code signal power.

The second coexisting existing signal simulated as a potential interferer was the current GPS P-Code signal. This signal was generated as depicted in Figure 3.7. The coexisting signal was generated with a random binary message which was BPSK modulated. The BPSK data modulated signal was then spread with a pseudorandom binary waveform at a 1.023 MHz chip rate. The spread BPSK signal was finally modulated to 20.23 MHz, the same center frequency as the simulated M-Code signal. This signal was inserted into the M-Code system as one of the interfering signals as shown in Figure 3.2.

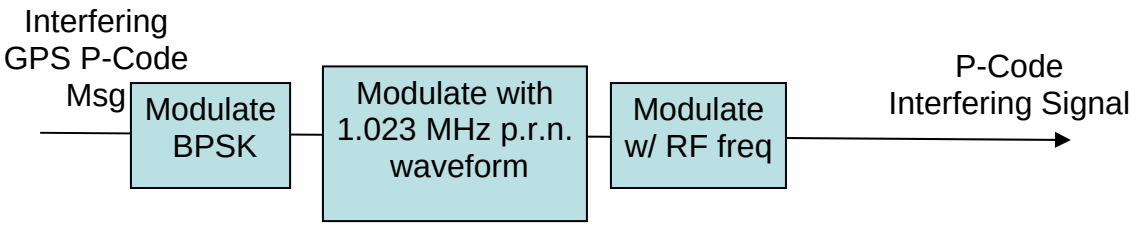

Figure 3.7: Block diagram of GPS P-Code interference generation. The 1.023 MHz pseudorandom noise chip rate reflects the actual bandwidth generated by the GPS satellites in orbit. The simulated P-Code was modulated to an RF frequency of 20.23 MHz, which is the same center frequency as the simulated M-Code signal.

The GPS P-Code interfering signal was initially modeled as coexisting with the M-Code signal and having the same received power. The received P-Code signal power was progressively increased in 2.0 dB steps to 80.0 dB above the received M-Code power level. Figure 3.8 depicts the worst case overlay of the power spectral densities of the M-Code signal and the GPS P-Code interferer, when the interfering signal is received with a +80.0 dB power level. Note: the BOC(10,5) spectral design of the M-Code signal places an M-Code signal null in the primary power lobe of the C/A-Code signal. The designed avoidance of the interfering signal complements the inherent signal rejection techniques inherent in direct sequence spread system coded systems.

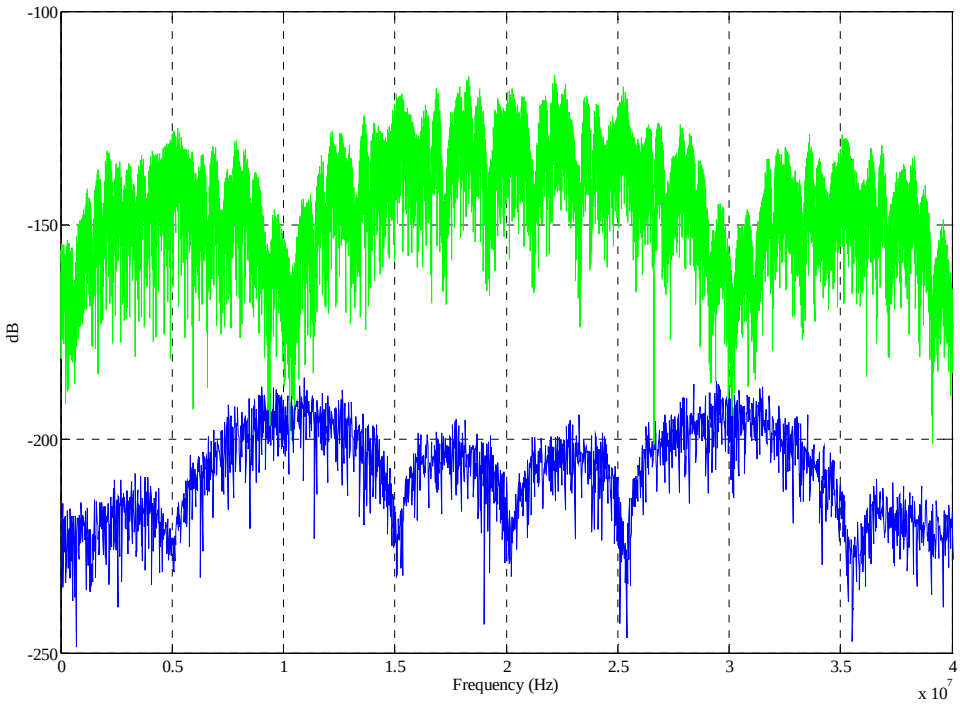

Figure 3.8: The PSDs of the M-Code signal (lower plot) and the coexisting P-Code signal (upper plot). Relative power levels depicted in this figure are for a worst case interfering scenario where the received P-Code signal power is 80.0 dB above the received M-Code signal power.

3.2.3 Simulated OFDM System Model

Orthogonal Frequency Division Multiplexing (OFDM) is a frequency division multiplexing modulation technique for transmitting large amounts of digital data. OFDM works by splitting the radio signal onto multiple smaller subcarriers that are then transmitted simultaneously at different frequencies in parallel to the receiver. For example, 802.11a WLAN, 802.16 and WiMAX technologies use OFDM. A generic block diagram for generating an OFDM signal is shown in Figure 3.9. In the simulation, a randomly generated sequence of data bits was modulated using 16-QAM (four bits per

QAM symbol). The input bit sequence was spread across 10 subcarriers which were simultaneously transmitted over the same frequency range as the M-Code signal and centered at 20.23 MHz.

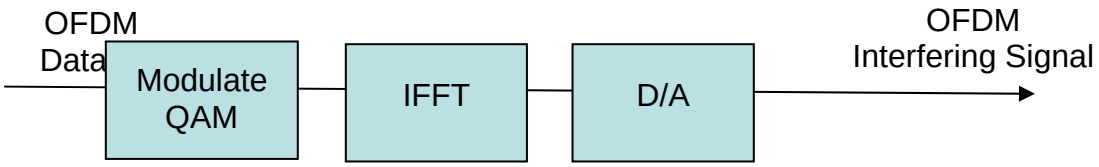

Figure 3.9: Block diagram of an OFDM signal generation. In the simulation, a randomly generated sequence of data bits was modulated using 16-QAM. This sequence was separated into 10 subcarriers which were transmitted simultaneously over the same frequency range as the M-Code signal and spectrally centered at 20.23 MHz.

The constellation map (bit-to-waveform mapping) for 4-bit 16-QAM modulation is shown in Figure 3.10. This bit stream is commonly used in 802.11a OFDM modulation [14].

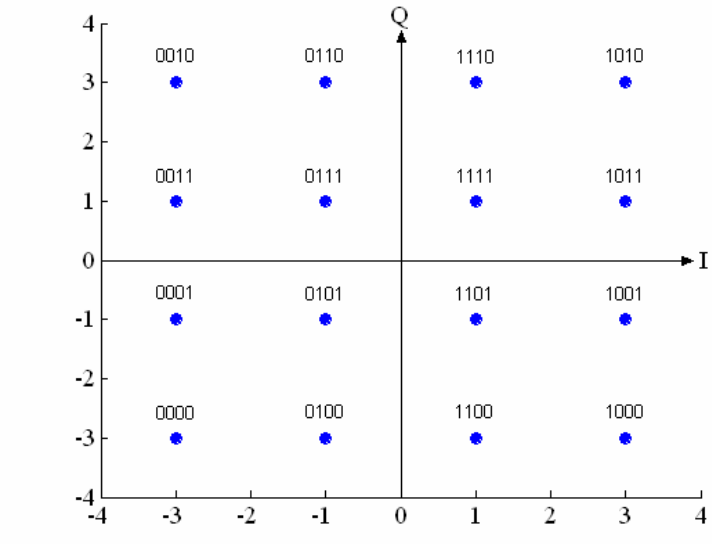

Figure 3.10: Constellation map for a 16-QAM modulated bit stream.

For this work, the OFDM signal was generated using an $N_{IFFT} = 128$ point IFFT. The subcarrier spacing was determined by $(N_{IFFT} \times f_s)^{-1}$ where f_s is the sample frequency. Using a simulated sample frequency of $f_s = 480 \times 10^6$ generates a subcarrier spacing of 3.75 MHz. A worst-case OFDM interfering signal using 10 subcarriers was developed. This OFDM signal contained all interfering power over 37.5 MHz of the simulated 40 MHz M-Code spectrum.

The OFDM signal can be represented by [15]:

$$c(t) = \sum_{n=0}^{N-1} m_n(t) \sin(2\pi n t), \tag{3.6}$$

where N is the number of subcarriers, $m_n(t)$ is the signal strength of each subcarrier, and n is the subcarrier frequency index. The IFFT is commonly expressed as [15]:

$$X(n) = \sum_{n=0}^{N-1} x(k) \sin(2\pi k n / N) - j \sum_{n=0}^{N-1} x(k) \cos(2\pi k n / N). \tag{3.7}$$

The OFDM interfering signal was initially modeled as a coexisting signal having the same received power level as the M-Code signal. The received OFDM signal power was progressively increased in 2.0 dB steps to a total of 80.0 dB above the received M-Code power level. Figure 3.11 depicts the worst case scenario whereby the interfering OFDM signal power is +80.0 dB above the received M-Code power level.

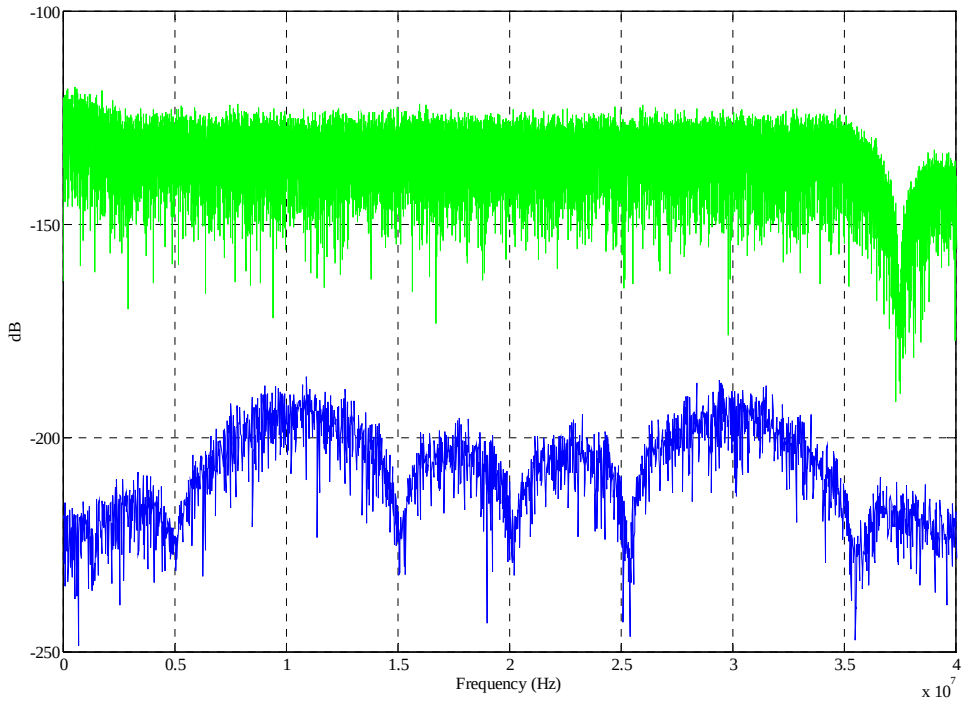

Figure 3.11: The PSDs of the M-Code signal (lower plot) and the coexisting OFDM signal (upper plot). Relative power levels depicted in this figure are for a worst case interfering scenario where the received OFDM signal power is 80.0 dB above the received M-Code signal power. To achieve perfect spectral coincidence, the OFDM center frequency was simulated at 20.23 MHz. Note: the 10 OFDM subcarrier responses distinctly appear in higher resolution plots but do not appear when using this larger amplitude scale.

3.2.4 Observed Interfering Signal Model

Although the exact modulation of the observed interfering signal is unknown, critical information can be interpreted from the power spectral density plot depicted in Figure 2.5. The peak amplitude of the interfering signal has a magnitude approximately 45.0 dB above the thermal noise floor and is centered approximately 4.0 MHz above the GPS L1 center frequency of 1575.42 MHz. For simulation purposes, the interfering

signal was assumed to be BPSK modulated in the absence of any other information; however, the specific interfering modulation will have only minor impact on the interference simulation. The actual power spectrum of the coexisting signal, relative to the M-Code signal, is the main driving factor in interference generation.

Using the following equations and the 45.0 dB receiver processing gain over the noise floor, the power level of the interfering signal *(I_P)* can be derived as shown in the following equations using *Average Noise Power* (*N_{AV})* defined as [15]

$$N_{Av} = N_o \times W_{RF} \quad \Rightarrow \quad N_o/2 = N_{Av}/\left(2 \cdot W_{RF}\right), \tag{3.8}$$

where $N_o/2$ is the two-sided noise PSD and W_{RF} is the RF bandwidth. Using (3.8) and accounting for 45.0 dB of receiver processing gain, interfering noise power I_P is given by

$$I_P = N_{Av}/\left(2 \cdot W_{RF}\right) + 10^{4.5}, \tag{3.9}$$

where for this work $N_{AV} = 7.94 \times 10^{-12}$ (determined by an estimated noise floor of -111.0 dB based on [7]) and $W_{RF} = 20.23\ MHz$ (down-converted M-Code RF filter bandwidth).

The interfering signal was modeled as a coexisting BPSK signal having the same received power level of 45.0 dB above the M-Code signal. Because the actual received power level of this signal does not vary (assuming a fixed/stationary observation point), the simulated power level of this signal remained fixed. Unlike previous interference simulations, the purpose of this simulation was not to determine the power level(s) at which the coexisting signal interfered with the M-Code signal. Rather, the goal was to determine if the signal would degrade the M-Code signal at the observed power level,

just as it does for the existing GPS signals. Figure 3.12 shows simulated PSDs for the M-Code signal and the modeled BPSK interferer.

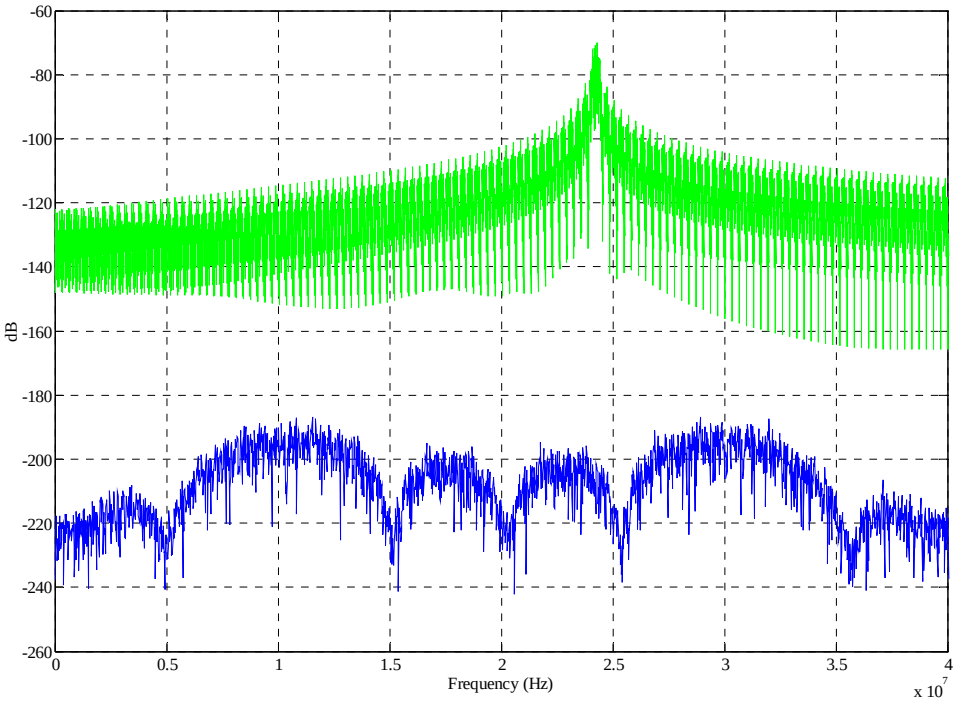

Figure 3.12: The PSDs of the M-Code signal (lower plot) and an observed interfering signal (upper plot). This figure depicts the interfering signal transmitted with a power level 45.0 dB greater than the noise floor (not shown). The center frequency of the coexisting interfered was simulated at 4.0 MHz above the simulated M-Code frequency of 20.23 MHz.

3.2.5 Interference Channel Model

The simulated M-Code system consists of the M-Code signal itself, the variable power interfering signal, and AWGN emulating channel noise. The M-Code signal power and noise power level were fixed to produce a constant SNR which yields a

specific P_B for the communications system. As shown earlier, SNR and E_b/N_o are equal for BPSK modulation with proper parameter selection. In this case, the conventional E_b/N_o vs. P_B plots for digital communications system can be depicted as SNR vs. P_B for the simulated BPSK systems. As interfering power levels are increased, the interference effects are characterized through the increasing P_B relative to the baseline performance. Relative to the received M-Code power, interfering power was increased from 0 dB to 80.0 dB above the M-Code power level in 2.0 dB steps with P_B calculated for each change in power.

3.3 Evaluation Metrics

The SNR provides a measure of the amount of unwanted electromagnetic noise present relative to the signal strength. If the background noise on a channel becomes higher than the signal, or insufficient receiver processing gain exists to compensate, it can cause a reduction in data speed or a disruption in system functionality [17].

The two evaluation metrics used to evaluate the potential interference of noise and the coexisting signals for the simulation are the *Average Interference Power*-to-*Average Signal Power* ratio (I/S) and *Average Signal Power*-to-*Average Interference-plus-Noise Power* Ratio (SINR). The *I/S* ratio is calculated as the ratio of the unwanted coexisting signal which degrades the receiver to the desired signal. The decibel (dB) form of *I/S* is

$$I/S_{(dB)} = 10 \times \log_{10}\left(\frac{P_{Coexisting\ Signal}}{P_{M-Code\ Signal}}\right). \tag{3.10}$$

The SINR is calculated as a ratio of *Average Signal Power*-to-*Average Interference-plus-Noise Power* where the interference power is from coexisting signals. The decibel (dB) form of SINR is

$$SINR_{(dB)} = 10 \times \log_{10}\left(\frac{P_{M-Code\ Signal}}{P_{Coexisting\ Signal} + P_{Noise}} \right). \tag{3.11}$$

Intuitively, given constant AWGN and M-Code signal powers, increasing the coexistent interfering signal power increases the *I/S* ratio and decreases the SINR.

IV. Results and Analysis

4.1 Interference Effects Overview

As in any communications system, spectrally coexistent signals can cause interference given sufficient interfering power is received. The interference rejection qualities of spread spectrum signals significantly decrease the interference effects of non-spread coexisting signals through rejecting a majority of interfering signals by the despreading and filtering operations. The key question in this study is whether the interference rejection capabilities of spread spectrum systems also apply to other coexisting signals operating at/near similar center frequencies and bandwidths.

A measure of the expected interference rejection, also known as receiver processing gain (G_p), of a spread spectrum signal is defined by [15] $G_p = W_{SS} / W_{min}$, where W_{SS} is the *spread spectrum bandwidth* and W_{min} is the *minimum system bandwidth*. For direct sequence systems, W_{ss} is approximately the Code chip rate, $R_{ch,}$ and W_{min} is similarly the data rate R. As a result, the processing gain of the simulation can be defined as $G_p = R_{ch} / R$ [15]. In this work, the theoretical M-Code processing gain was calculated using the filter bandwidths as $G_p = W_{RF\_filt} / W_{BB\_filt} = 2\times(10.23\times10^6) / 20{,}460$ or 30.0 dB. This calculation suggests that the simulated M-Code system should reject approximately 30.0 dB of combined interference and noise power before the bit error rate significantly degrades (increases).

For the C/A-Code, P-Code, and OFDM interfering signals, the power levels were initially set at the same level as the M-Code signal and then gradually increased up to

80.0 dB, well past the expected power level causing the bit error rate to reach 50%. The calculated *I/S* and SINR analysis, as power is increased, demonstrated the susceptibility and, therefore, rejection of the M-Code signal to these types of coexisting interferers.

4.2 Interference Effects: Current C/A-Code Signal

The first signal that was generated to examine its interference effects while coexisting with the simulated M-Code signal was the GPS C/A-Code. Figure 4.1 and Figure 4.2 show P_B versus *I/S* and SINR as current GPS C/A-Code signal power increases from 0.0 dB to 80.0 dB above the received M-Code power with the M-Code system SNR fixed at -39.0 dB.

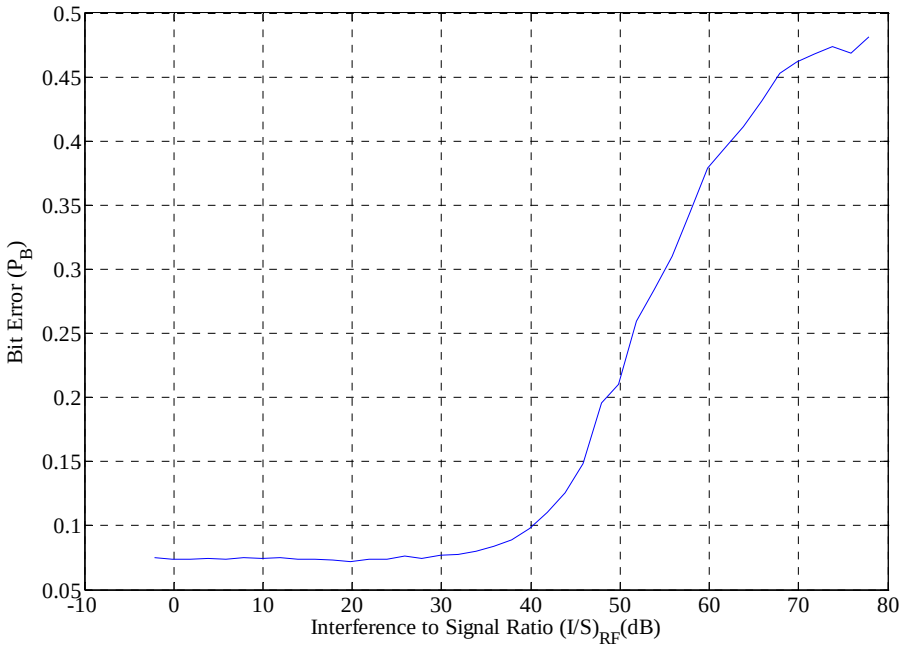

Figure 4.1: The P_B vs. *I/S* ratio for GPS C/A-Code coexisting with the M-Code. The plot shows P_B increases as interfering power increases to 80 dB above received M-Code power.

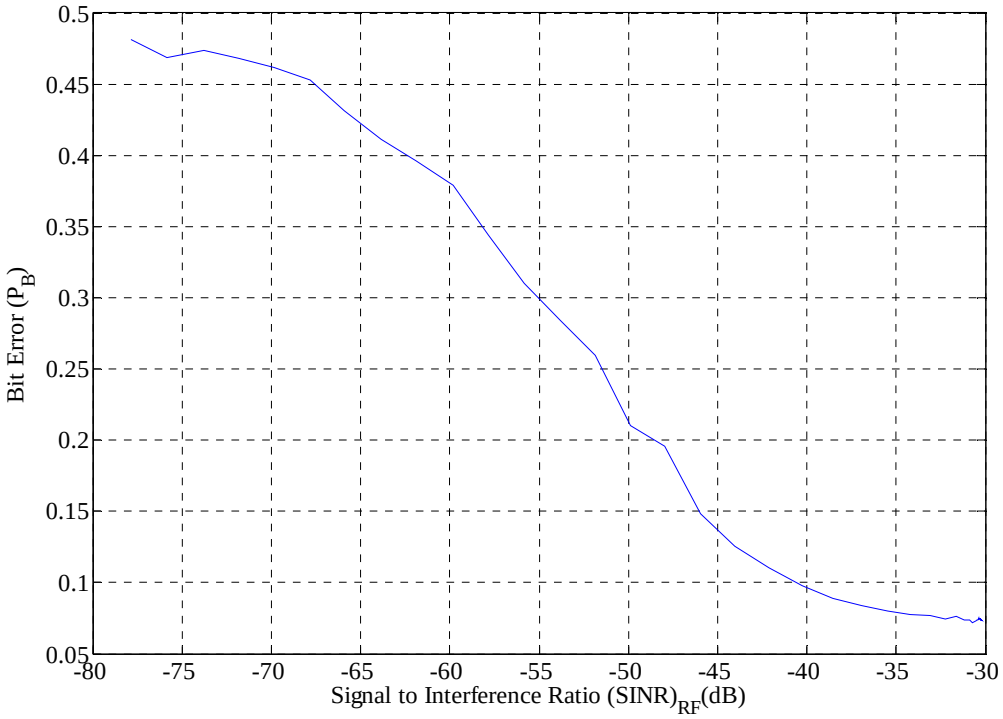

Figure 4.2: The P_B vs. SINR for GPS C/A-Code coexisting with the M-Code. The plot shows P_B increases as interfering power increases to 80 dB above received M-Code power.

4.3 Interference Effects: Current P-Code Signal

The second signal that was generated to examine its interference effects while coexisting with the simulated M-Code signal was the GPS P-Code. Figure 4.3 and Figure 4.4 show P_B versus *I/S* and SINR as current GPS P-Code power increases from 0.0 dB to 80.0 dB above the received M-Code power with the M-Code system SNR fixed at -39.0 dB.

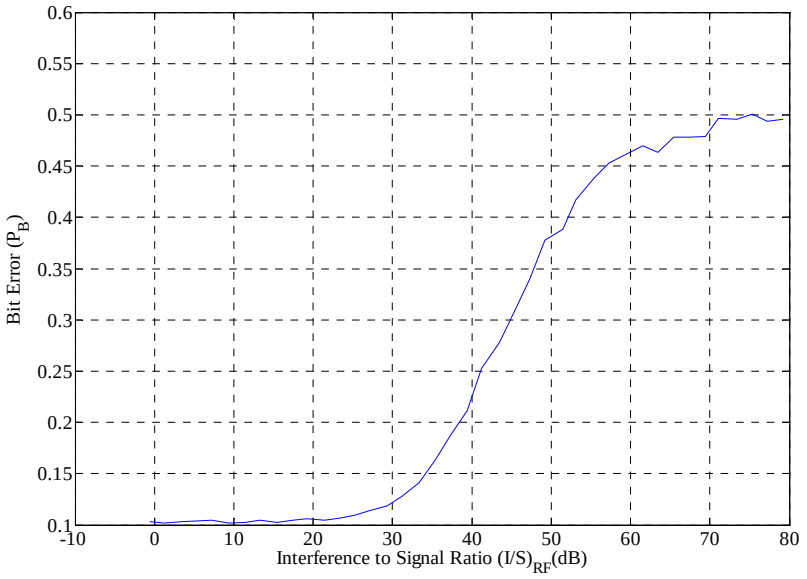

Figure 4.3: The P_B vs. *I/S* ratio for GPS P-Code coexisting with the M-Code. The plot shows P_B increases as interfering power increases to 80.0 dB above received M-Code power.

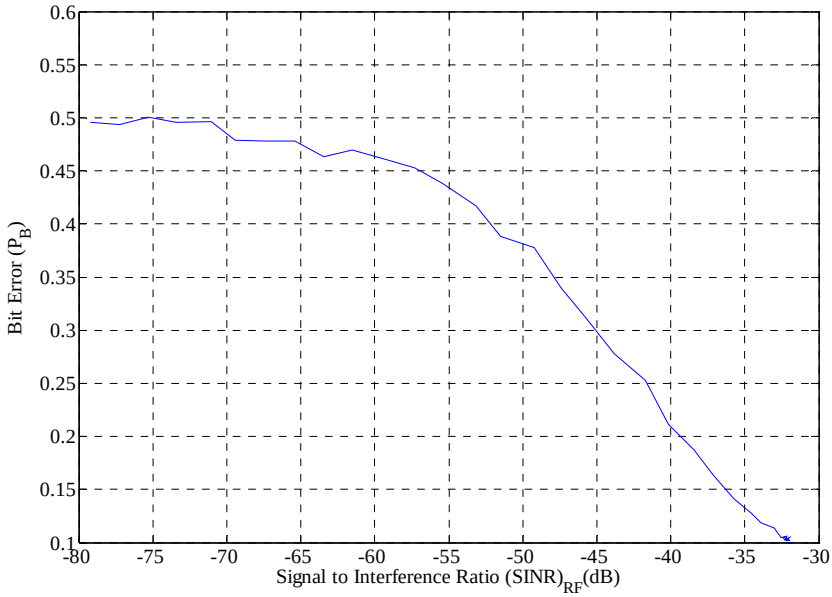

Figure 4.4: The P_B vs. SINR for GPS P-Code coexisting with the M-Code. The plot shows P_B increases as interfering power increases to 80.0 dB above received M-Code power.

4.4 Interference Effects: OFDM Signal

The third interfering signal that was generated as a worst-case OFDM signal centered on the M-Code carrier with all of its power contained within the M-Code bandwidth. Figure 4.5 and Figure 4.6 show P_B versus *I/S* ratio and SINR as OFDM interfering power increases from 0.0 dB to 80.0 dB above the received M-Code power with the M-Code system SNR fixed at -39.0 dB.

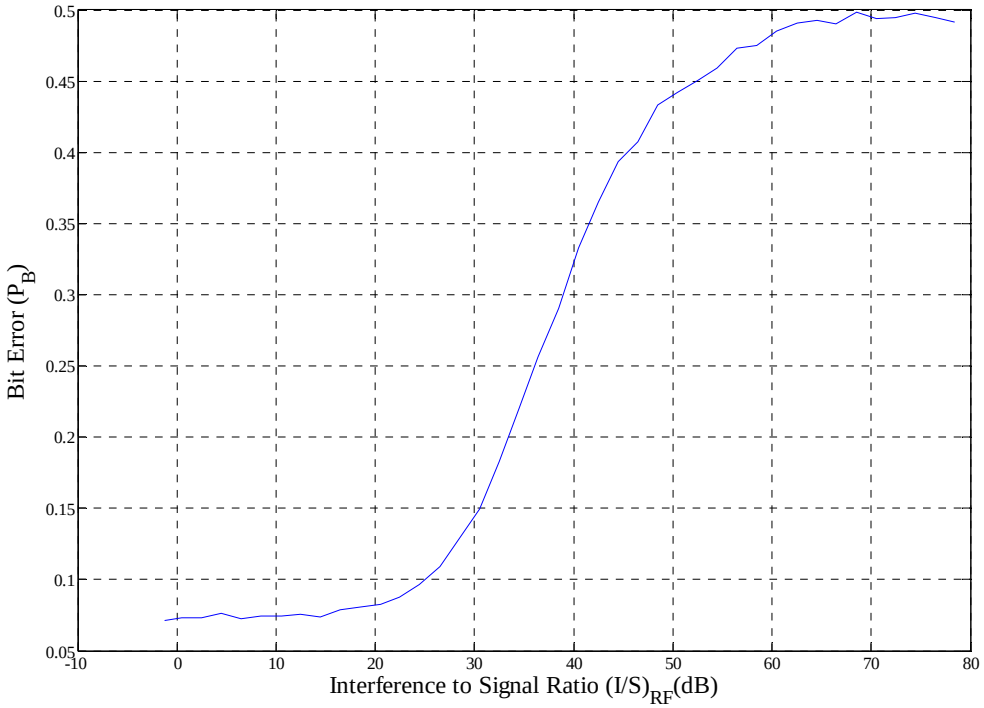

Figure 4.5: The P_B vs. *I/S* ratio for OFDM signal coexisting with the M-Code. The plot shows P_B increases as interfering power increases to 80.0 dB above received M-Code

power.

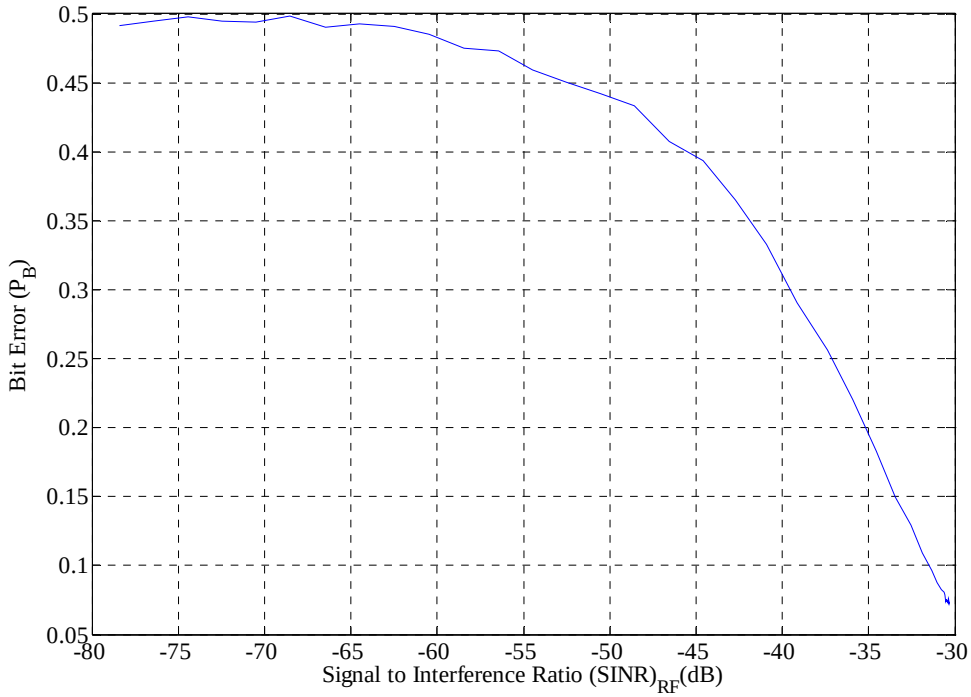

Figure 4.6: The P_B vs. SINR for OFDM signal coexisting with the M-Code. The plot shows P_B increases as interfering power increases to 80.0 dB above received M-Code power.

4.5 Interference Effects: Observed Signal

It has been repeatedly observed that the actual coexisting signal shown in Figure 2.5 causes so much interference in the L1 spectrum that current GPS C/A-Code and P-Code receiver performance is degraded to a total loss of signal within the immediate vicinity of the transmitter. To determine whether or not this same signal will degrade future M-Code performance, the M-Code system was simulated with the interference effects present. Figure 4.7 shows a relatively constant bit error rate of approximately 50% over the 6 dB simulated power range. The results confirm that the

interfering L1 signal will disrupt the M-Code signal, just as it currently corrupts the GPS L1 C/A-Code and P-Code receiver performance.

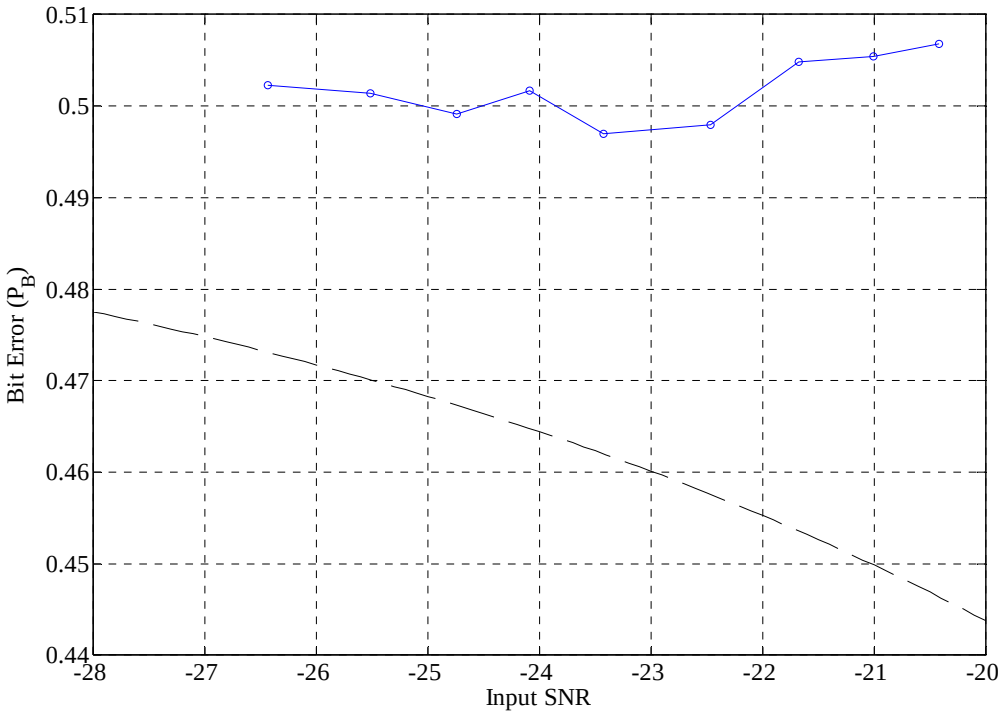

Figure 4.7: The P_B vs. SNR for M-Code coexisting with observed interfering signal. Interfering signal power was varied ± 3.0 dB about observed power levels. Simulated P_B was compared with theoretical for BPSK system as defined in (3.1).

4.6 Simulation Results

Significant differences in the *I/S* ratio were observed with the simulated coexistence of the M-Code BOC signal with C/A-Code, P-Code, and OFDM signals when the M-Code SNR was fixed. In each case, bit error rate, P_B of the *I/S* ratio started at an initial P_B determined by the system SNR. As the relative power level of the

coexisting signal was increased, the P_B initially stayed constant, but eventually increased as the coexisting signal gain caused escalating interference. The interference caused the P_B to eventually approach a maximum of 50%. This result makes intuitive sense; initially, the interference rejection characteristics inherent in spread spectrum systems prevent an increase in P_B, but eventually, a point is reached where the interference from the coexisting signal produces escalating estimation errors.

The amount of signal power required to cause interference differed between the coexisting signals. Table 4.1 compares the amount of coexisting signal power required to interfere with the M-Code system enough to degrade the *I/S* ratio P_B to representative probabilities of 0.15, 0.30, and 0.45. As shown, a coexisting C/A-Code signal requires a received power level which is 48.0 dB above the received M-Code signal to cause sufficient interference for P_B to reach 0.15. Conversely, a coexisting OFDM signal requires a received power level of only 32.0 dB above the received M-Code signal to cause sufficient interference for P_B to reach 0.15. Overall, data in Table 4.1 suggests that the coexisting OFDM signal requires less power to degrade the M-Code P_B performance (to a specified level) than either the C/A-Code or P-Code signals. These *I/S* results suggest that the M-Code system is most susceptible to OFDM interference.

Table 4.1: *I/S* ratio results for signals coexisting with the M-Code signal

***I/S* BER Results**			
P_B	**Coexisting Signal Power Delta (dB)**		
	C/A-Code	**P-Code**	**OFDM**
0.15	48.0	35.0	32.0
0.30	57.0	45.0	40.0
0.45	70.0	58.0	54.0

Similarly to the *I/S* analysis, diversity was shown by the SINR results between the different signals coexisting with the M-Code BOC signal. In each case, the probability of bit error, P_B, of the SINR started at approximately 50%. As the relative power level of the M-Code signal was increased, the P_B initially stayed constant, eventually decreasing as the increasing power of the desired signal produced an increasingly correct probability of BPSK bit estimation. The P_B eventually approach a minimum probability determined by the system SNR. This result also makes intuitive sense; initially, the M-Code signal is totally overwhelmed by the interference from the coexisting signals and environmental noise, causing the maximum possible error rate; eventually, the power of the desired signal is increased to a level where it is able to overcome the organized interference of the coexisting signal, stabilizing at the minimum P_B dictated by the M-Code system noise.

The amount of signal power required to cause significant changes to the SINR differed between the coexisting signals. Table 4.2 compares the amount of coexisting signal power required to interfere with the M-Code system enough to generate SINR representative P_B probabilities of 0.15, 0.30, and 0.45. As shown, an M-Code signal can coexist with a C/A-Code signal at a transmission power level of -46.0 dB below the interferer and noise with a P_B of 0.15. In contrast, an M-Code signal coexisting with an OFDM signal generates an SINR P_B of 0.15 only -33.0 dB below the interferer and noise. Again, supporting the *I/S* ratio conclusions, OFDM coexisting signals require less power to degrade the M-Code P_B than either than C/A-Code or P-Code systems.

Table 4.2: SINR results for signals coexisting with the M-Code signal

SINR BER Results			
P_B	Coexisting Signal and Noise Power Delta (dB)		
	C/A-Code	P-Code	OFDM
0.15	-46.0	-37.0	-33.0
0.30	-55.0	-45.0	-39.0
0.45	-67.0	-57.0	-52.0

Finally, the SNR vs. Bit Error curve on Figure 4.7 displays the interference effects of the actual interfering signal on the M-Code system. The data points display a relatively constant bit error rate of approximately 50% over the 6 dB simulated power range. The slight variation is simply due to statistical inaccuracies caused by the error counting subroutine; this variation could be reduced through a longer simulation. Any possibility of correct signal detection would have been demonstrated by the data points tracking relatively parallel to the theoretical curve. The results confirm that the interfering L1 signal will disrupt the M-Code signal, just as it currently corrupts the GPS L1 C/A-Code and P-Code receiver performance.

4.6 Summary

This chapter provides the results and analysis of the GPS M-Code signal coexisting with various other waveforms. Degradation analysis was performed through examining the bit error performance of the Interference-to-Signal (*I/S*) ratio and Signal-to-Interference-plus-Noise-Ratio (SINR) plots. The discussion is based on comparison of

baselined M-Code system performance to the performance with interferers present when the M-Code SNR is fixed at -39.0 dB. Interferers include the current GPS C/A-Code and P-Code signals, designed to coexist on the same L1 frequency bandwidth, as well as a theoretically worst-case OFDM signal designed to maximize confliction with the primary M-Code frequency band. Additionally, potential interference effects of a real-world signal which currently interferes with the GPS L1 C/A-Code and P-Code were simulated for the M-Code system to determine if interference was likewise probable.

An *I/S* ratio analysis indicates that the GPS C/A-Code signal causes the least interference with the M-Code signal and that the OFDM signal produces the most interference under equal interference power conditions. The C/A-Code signal can be received with 48.0 dB higher power than the M-Code signal before the M-Code system bit error rate degrades to $P_B = 0.15$. The C/A-Code signal requires a 70.0 dB power delta before the M-Code error rate approaches a near-maximum value $P_B = 0.45$. Results also show that the M-Code system is more susceptible to interference from a P-Code signal, as a 35.0 dB power delta is required to degrade the M-Code performance to $P_B = 0.15$. The M-Code signal is most susceptible to interference from a coexisting OFDM signal. For an OFDM interfering signal, only a 32.0 dB received power delta is required to degrade M-Code bit error rate to $P_B = 0.15$. M-Code performance degrades to $P_B = 0.45$ when the interfering OFDM power delta reaches 54.0 dB.

Examination of the SINR data exhibits very similar results: the GPS C/A-Code signal causes the least interference with the M-Code signal and the OFDM signal produces the most interference given equivalent received power conditions. An M-Code

signal can coexist with a C/A-Code signal at a received power level of 46.0 dB below the interferer (-46.0 dB) and noise with $P_B = 0.15$. The M-Code signal requires a -67.0 dB C/A-Code interference-plus-noise-power delta before the M-Code P_B is increased to a near-maximum value of $P_B = 0.45$. Results also show that the M-Code system is more susceptible to interference from a P-Code signal, as a SINR power delta of -37.0 dB is required to degrade the M-Code performance to $P_B = 0.15$. The M-Code signal is most susceptible interference from the OFDM coexisting signal where only a -33.0 dB SINR power delta causes the M-Code error rate to reach $P_B = 0.15$; the M-Code performance is degraded to a $P_B = 0.45$ for an OFDM SINR power delta of -52.0 dB.

The final simulation verified that a specific BPSK signal with a received power level 45 dB greater than the noise floor, in the M-Code bandwidth, will completely corrupt reception of the M-Code signal as it currently disrupts reception of the L1 C/A-Code and P-Code signals today. The interference from the signal will overwhelm the desired M-Code signal, degrading the reception of the desired signal to be unusable in the local area. The data displays a relatively constant error rate of $P_B \cong 0.5$ over a power range of ± 3.0 dB around the observed power level. The results confirm that the interfering observed signal will disrupt M-Code performance, just as it currently corrupts the GPS L1 C/A-Code and P-Code signals.

V. Conclusions and Recommendations

5.1 Conclusions

This research presented modeling, simulation, and analysis results for characterizing Binary Offset Carrier (BOC) system performance in the presence of four interfering signals. Within this effort, BOC performance is characterized using a basic system model and parameters consistent with those of the GPS Military System (M-Code signal). The interfering signals evaluated included: 1) the direct sequence spread spectrum (DSSS) GPS clear/acquisition (C/A-Code) signal, 2) the DSSS GPS precision (P-Code) signal, 3) an Orthogonal Frequency Division Multiplexed (OFDM) signal, and 4) an observed interfering signal collected insitu at a site in Southern California. All interfering signals were modeled as being spectrally coexist within the same bandwidth as the M-Code signal. Interference effects were characterized by comparing the bit error performance of a simulated M-Code system; first independently, and then coexisting with the other interfering signals. Modeling, simulation and analysis results are based on the following key assumptions:

- The interference effects demonstrated are for a single M-Code receiver system with a single interfering signal and AWGN present.
- The M-Code system performance was characterized at a down-converted frequency of 20.23 MHz versus the actual L1 and L2 RF frequencies of 1575.42

MHz and 1227.6 MHz, respectively. Conclusions based on this simulation are still applicable to actual L1 and L2 transmission frequencies.

- The M-Code system performance was characterized using a simulated data rate of 20,460 bits/second versus the actual M-Code message rate of 50 or 200 bits/second. Conclusions based on this simulation are still applicable to actual M-Code data message rates.
- Both the desired M-Code signal and the interferers are received along a direct line-of-sight from their transmission sources and experience identical processing upon reception.

Simulation results indicate that current GPS C/A-Code and P-Code signals will have negligible impact on M-Code system performance at the minimum M-Code received power level of -160.0 dBW when these signals are received at their minimum received power levels of -160.0 dBW and -163.0 dBW, respectively. Both the GPS C/A-Code and P-Code signals can exceed the M-Code received power by over 35 dB before M-Code system performance is significantly degraded.

The M-Code system is very tolerant to coexisting C/A-Code signals. As an example, *Average Interference Power*-to-*Average Signal Power (I/S)* ratio characterization demonstrates that a C/A-Code signal 48.0 dB greater than the M-Code signal degrades performance to $P_B = 0.15$. The M-Code system interference is maximized when the C/A-Code signal is received at 70.0 dB greater signal strength than the M-Code signal.

The M-Code system is more sensitive to interference from coexisting P-Code signals. The *I/S* characterization demonstrated that a P-Code signal at 35.0 dB greater than the M-Code signal degrades performance to $P_B = 0.15$. The M-Code system interference is maximized when the P-Code signal is received at 58.0 dB greater signal strength than the M-Code signal.

The OFDM interference results indicate that the M-Code system is significantly more sensitive to coexistence with a signal of this type for the wideband systems simulated. The *I/S* ratio characterization demonstrates that an OFDM signal 30 dB greater than the M-Code signal degrades performance to $P_B = 0.15$. The M-Code system interference is maximized when the OFDM signal is received at 54.0 dB greater signal strength than the M-Code signal.

The difference in interference results between the C/A-Code signal, the P-Code signal, and the OFDM signal is expected. The C/A-Code coexisting signal has a much smaller bandwidth than the M-Code signal, occupying a minority of the M-Code RF filter bandwidth, thus contributing a small amount of interfering power to the M-Code system. The P-Code coexisting signal has the same bandwidth the M-Code signal, fully occupying the M-Code RF filter bandwidth but with a power level that decreases away from the RF center frequency, thus contributing a moderate amount of interfering power to the M-Code system. The OFDM coexisting signal has the same bandwidth the M-Code signal, fully occupying the M-Code RF filter bandwidth with a relatively constant power level, thus contributing a significant amount of interfering power to the M-Code system. Based on this examination of the interfering power that enters that M-Code RF

filter, the C/A-Code, P-Code, and OFDM coexisting signals will intuitively cause relatively increasing amounts of interference.

Final simulation results verified that a specific BPSK signal (model based on an observed interfering signal in southern California) with a received power level 45.0 dB greater than the noise floor in the M-Code bandwidth completely corrupts reception of the M-Code signal just as it disrupts reception of the C/A and P-Code L1 signals today. These results demonstrate that the M-Code system can be susceptible to the same non-wideband interferers as the C/A-Code and P-Code systems.

5.2 **Recommendations for future research**

Several assumptions were used when constructing the models for this research. Relaxing some of the imposed restrictions should be considered to develop possible topics for follow-on research to more fully explore the potential interference effect of BOC systems with coexisting with other signals. Potential follow-on topics include:

1. Modeling, simulation, and analysis could be conducted using a larger number of simultaneously coexisting C/A-Code and P-Code signals as interferers. The GPS constellation is comprised of 24+ satellites and thus there are multiple (uniquely coded) interfering signals received at any given time. A recommendation is to use this many sources as potential interferers, as well as a combination of C/A-Code and P-Code signals simultaneously.
2. Consideration could be given to running simulations at actual L1 and L2 RF transmission frequencies using actual M-Code data rates. Such simulations

would incorporate “coloration” effects induced as a result of additional mixing and filtering which were not considered in this work.

3. The interference effects of other modern signals (communication, navigation, radar, etc.) on M-Code system performance could be evaluated. Other signals exist internationally [18, 19] which could impact M-Code system performance on the L1 or L2 bands. The down-converted model developed and analyzed here allows virtually any interfering waveform to be easily incorporated and its effect on detection performance characterized.

Bibliography

1. Barker, Brian C. and others. "Overview of the GPS M Code Signal." *Proceedings of Institute of Navigation, 2000 National Technical Meeting*. Alexandria VA: Institute of Navigation, 2000.

2. Hein, Guenter W. and others. "Status of Galileo Frequency and Signal Design." *Proceedings of Institute of Navigation, 2002 National Technical Meeting*. Alexandria VA: Institute of Navigation, 2002.

3. Betz, John W. "Analysis of M-Code Interference with C/A-Code Receivers." *Proceedings of Institute of Navigation, 2000 National Technical Meeting*. Alexandria VA: Institute of Navigation, 2000.

4. NAVSTAR GPS Joint Program Office (JPO). *Navstar GPS Space Segment/Navigation User Interfaces*. Interface Control Document. El Segundo, CA: GPS JPO, 1997.

5. UWB Forum Home Page. October 28, 2005 http://www.uwbforum.org/.

6. Haykin, S. "Cognitive Radio: Brain-Empowered Wireless Communications." *IEEE Journal in Selected Areas of Communications*. Vol. 23, No. 2, Feb 2005, pp. 201-220.

7. Do, Ju-Yong and others. "L and S Bands Spectrum Survey in the San Francisco Bay Area." *IEEE Position Location and Navigation Symposium (PLANS) 2004*. Apr 2004, pp 566-572.

8. Geier, Jim. "Enabling Fast Wireless Networks with OFDM." (February 2001) September 10, 2005 http://www.commsdesign.com/story/OEG20010122S0078

9. Backscheider, R.J. "Ultra Wide Band Signal Modeling for Radar Receiver Characterization." Wright-Patterson AFB, OH. AFIT/GE/ENG/04-28.

10. NAVSTAR GPS Joint Program Office (JPO). *Navstar GPS Military-Unique Space Segment/User Segment Interfaces*. Interface Control Document. El Segundo, CA: GPS JPO, 2001.

11. NAVSTAR GPS Joint Program Office (JPO). *Global Positioning System Standard Positioning Service Signal Specification*, (2nd Edition). El Segundo, CA: GPS JPO, 1995.

12. Zogg, J.M. "GPS Basics: Introduction to the System--Application Overview." (March 26, 2002). August 9, 2005 http://www.u-blox.com.

13. NAVSTAR GPS Joint Program Office (JPO). *NAVSTAR GPS User Equipment Introduction*. El Segundo, CA: GPS JPO 1996.

14. LAN/MAN Standards Committee of the IEEE Computer Society. "Part 11: Wireless LAN Medium Access Control (MAC) and Physical Layer (PHY) specifications--High-speed Physical Layer in the 5 GHz Band." *IEEE Std 802.11a-1999(R2003)*. 2003.

15. Sklar, Bernard, *Digital Communications Fundamentals and Applications*, (2nd Edition): NJ: Prentice Hall PTR, 2003.

16. Holmes, J.K. and S. Raghavaen. "GPS Signal Modernization Update Summary." *Proceedings of Institute of Navigation 58th Annual Meeting/CIGTF 21st Guidance Test Symposium*. Alexandria VA: Institute of Navigation 2002.

17. Lee, Copeland., "Signal to Noise Ratio Quickstudy." (January 2001). August 9, 2005 http://computerworld.com/printthis/2001/0,4814,56253,00.html

18. Clynch, J.R. and others, "The Hunt for RFI: Unjamming a Coast Harbor." (January 2003). August 10, 2004 http://www.gpsworld.com.

19. Butsch, Felix. "A Growing Concern Radiofrequency Interference and GPS." (October 2002) July 12, 2004 http://www.gpsworld.com.

REPORT DOCUMENTATION PAGE

Form Approved
OMB No. 074-0188

PLEASE DO NOT RETURN YOUR FORM TO THE ABOVE ADDRESS.

1. REPORT DATE *(DD-MM-YYYY)*	**2. REPORT TYPE**	**3. DATES COVERED** *(From – To)*
22-12-2005	**Master's Thesis**	Jun 2004-Mar 2005

4. TITLE AND SUBTITLE

Characterization of Binary Offset Carrier (BOC) Systems Coexisting with Other Wideband Signals

5a. CONTRACT NUMBER

5b. GRANT NUMBER

5c. PROGRAM ELEMENT NUMBER

6. AUTHOR(S)

Hedenberg, John M., Major, USAF

5d. PROJECT NUMBER
If funded, enter ENR #

5e. TASK NUMBER

5f. WORK UNIT NUMBER

7. PERFORMING ORGANIZATION NAMES(S) AND ADDRESS(S)
Air Force Institute of Technology
Graduate School of Engineering and Management (AFIT/EN), Bldg. 640
2950 Hobson Way
WPAFB OH 45433-7765

8. PERFORMING ORGANIZATION REPORT NUMBER

AFIT/GE/ENG/06-02

9. SPONSORING/MONITORING AGENCY NAME(S) AND ADDRESS(ES)
AFRL/SNRW, Attn: Mr. James P. Stephens
2241 Avionics Circle, WPAFB OH 45433
937-255-5579 x3547 DSN: 785-5579 x3547
James.Stephens@wpafb.af.mil

10. SPONSOR/MONITOR'S ACRONYM(S)

11. SPONSOR/MONITOR'S REPORT NUMBER(S)

12. DISTRIBUTION/AVAILABILITY STATEMENT
APPROVED FOR PUBLIC RELEASE; DISTRIBUTION UNLIMITED

13. SUPPLEMENTARY NOTES

14. ABSTRACT

Results for modeling, simulation, and analysis of interference effects that modern interfering signals have on the system performance of the Binary Offset Carrier (BOC) signals, such as the Global Positioning System (GPS) Military System (M-Code signal) are addressed in this work. Three signals are addressed as potential interferers. These include the current GPS clear/acquisition code (C/A-Code) signal, the current GPS precision code (P-Code) signal, and an Orthogonal Frequency Division Multiplexed (OFDM) signal. All of these potential interferers are modeled as coexisting within the same bandwidth as the M-Code signal. Interference effects are characterized by comparing the bit error performance of a simulated M-Code system independently and then with the coexisting signal present. The results indicate that the GPS C/A-Code and P-Code signals can exceed the M-Code received power by over 25 dB before the M-Code system performance is degraded. The OFDM interference results indicate that the M-Code system is more sensitive to coexistence with a signal of this type; the M-Code system is significantly degraded with OFDM signals just over 30 dB stronger than the M-Code signal.

15. SUBJECT TERMS
GPS M-Code, Binary Offset Carrier (BOC), Interference, GPS Signal Generation, Spread Spectrum, Average Interference Power-to-Average Signal Power (I/S) ratio, Average Signal Power-to-Average Interference-plus-Noise Power Ratio (SINR).

16. SECURITY CLASSIFICATION OF:			**17. LIMITATION OF ABSTRACT**	**18. NUMBER OF PAGES**	**19a. NAME OF RESPONSIBLE PERSON**
REPORT	**ABSTRACT**	**c. THIS PAGE**			**Maj. Todd Hale**
U	**U**	**U**	**UU**	112	**19b. TELEPHONE NUMBER** *(Include area code)* (937) 255-3636 ext 4369

Standard Form 298 (Rev: 8-98)
Prescribed by ANSI Std. Z39-18